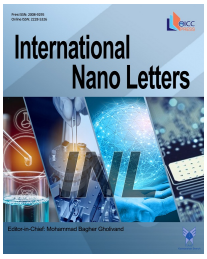

Volume 15, Issue 3, 152509 (1-22)

International Nano Letters (INL)

https://doi.org/10.57647/inl.2025.1503.09

Quantum Dot-Integrated Perovskite Solar Cells: A Pathway to Enhanced Light Harvesting and Stability

Promud Konch[1], Prerona Singha[1], Pradip Kumar Kalita[1,*], Sagar Bhattarai[2]

[1]*Department of Physics, Rajiv Gandhi University, Arunachal Pradesh, India.*
[2]*Technology Innovation and Development Foundations, Indian Institute of Technology Guwahati, Guwahati, Assam, India.*

[*]**Corresponding author:** pradip.kalita@rgu.ac.in

Original Research

Received:
4 July 2025
Revised:
10 August 2025
Accepted:
25 August 2025
Published online:
30 September 2025

Abstract:

Perovskite solar cells (PSCs) have emerged as a transformative photovoltaic technology, combining high power-conversion efficiencies with inexpensive, solution-based processing. However, their intrinsic instability and incomplete optical absorption currently hinder their widespread application. The integration of quantum dots (QDs) into PSCs has arisen as a promising strategy to address these limitations. By broadening the absorption spectrum, passivating defects, and facilitating charge transport, QDs can push single-junction PSC efficiencies to $\sim 26\%$ while improving long-term stability. This review surveys recent progress in QD-PSCs systems, covering QDs synthesis and incorporation methods, device architectures, and optoelectronic enhancements. We discuss the multifaceted roles of QDs in defect passivation, moisture resistance, and interface engineering, and highlight concerns about scalability and lead toxicity. Finally, we outline future directions such as lead-free QDs, tandem cell designs, and scalable manufacturing to position QD-enhanced PSCs as next-generation photovoltaic candidates.

Keywords: Quantum dots; Perovskite solar cells; Photovoltaic cells; Light harvesting; Defect passivation; Stability enhancement

Cite this article: Konch, P., Singha, P., Kalita, P.K., Bhattarai, S. Quantum Dot-Integrated Perovskite Solar Cells: A Pathway to Enhanced Light Harvesting and Stability. *Int. Nano Lett.* **15**(3), 152509 (2025).

1. Introduction

Solar energy offers a clean, sustainable means to satisfy the growing global energy demand and mitigate climate change. Among emerging photovoltaic (PV) technologies, perovskite solar cells (PSCs) have attracted tremendous attention due to their exceptional power-conversion efficiencies [1], low-cost solution-processable fabrication, and tunable optoelectronic properties. Typical PSCs utilize metal-halide perovskites with the formula ABX_3 (A = monovalent cation, B = divalent metal cation, X = halide) [2]. These perovskite materials combine very strong light absorption with long carrier diffusion lengths and high charge carrier mobilities attributes that are ideal for next-generation photovoltaics [2, 3]. Despite rapid improvements, PSCs remain highly unstable, being extremely sensitive to moisture, oxygen, heat, and UV light [4, 5], which induce structural degradation and performance loss. Moreover, single-junction PSCs cannot capture all wavelengths of sunlight, leaving a portion of the solar spectrum unharvested. Enhancing PSC durability and light-harvesting capability while retaining high efficiency is thus a critical challenge. To address these stability issues, we propose the integration of quantum dots (QDs) as a targeted strategy. QDs form a defect-passivating and moisture-resistant interface layer that shields the perovskite from environmental stressors and suppresses degradation pathways.

In this context, incorporating semiconductor quantum dots (QDs) into PSC architectures has emerged as a promising solution to simultaneously enhance PSC efficiency and stability. QDs are nanocrystals exhibiting strong quantum confinement effects, allowing their bandgaps and optical properties to be tuned by size [9]. When integrated into PSCs, QDs can serve multiple roles: they broaden light harvesting, passivate surface and bulk defects, improve charge separation, and suppress non-radiative recombination, all of

which contribute to higher efficiency and operational stability [10]. For instance, the hydrophobic ligands on certain QDs can repel moisture. Additionally, the tunable energy levels of QDs improve interfacial energy-level alignment and reduce deleterious charge accumulation, thereby mitigating the instability factors mentioned above. Researchers have explored various ways to integrate QDs into PSCs, including using QDs for surface passivation, embedding them in charge-transport layers, or even placing them directly in the perovskite absorber [11]. These strategies have already yielded significant performance boosts, with some QD-PSC devices demonstrating efficiencies that approach or potentially exceed the Shockley-Queisser limit [12].

The unique properties of QDs (size comparable to their exciton Bohr radius) give them a large specific surface area and discrete energy levels [13]. Unlike molecular additives, QDs offer enhanced thermal stability and higher carrier mobilities without introducing significant energy barriers to transport [14]. Their broad, size-tunable absorption and emission spectra allow efficient energy transfer into the perovskite layer [15]. Moreover, different classes of QDs have specific advantages: lead-halide perovskite QDs provide excellent energy level matching with the host absorber, while metal-chalcogenide and carbon-based QDs can improve environmental stability and reduce toxicity [16–18].

This review provides a comprehensive overview of QD-PSC systems. We first summarize the key QD materials used in PSCs (section 2), then describe the device characterization methods (section 3). We discuss interface engineering strategies enabled by QDs (section 4) and various device architectures including conventional, inverted, and tandem cells (section 5). Section 6 covers fabrication techniques for depositing QDs in PSCs. We then address scalability (section 7), operational stability (section 8), and toxicity concerns (section 9). Finally, we outline future outlooks (section 10) and provide concluding remarks (section 11).

2. Quantum dot materials for PSCs

Quantum dots (QDs) are instrumental in enhancing the efficiency and stability of PSCs by tailoring optical and electronic properties to optimize energy conversion [19]. Researchers have incorporated numerous types of QDs into PSCs, including perovskite-structured QDs, metal chalcogenide QDs, phosphorus-based QDs, carbon-based QDs, and metallic QDs [21–24]. In addition, atomically thin materials such as molybdenum disulfide (MoS_2) and MXene QDs have been explored for device enhancement. Among these, the most commonly used QD materials in PSC architectures are lead halide perovskite QDs, metal chalcogenide QDs, and carbon-based QDs, owing to their favorable optoelectronic properties and compatibility with perovskite films.These QDs are typically synthesized using methods such as hot-injection, ligand-assisted reprecipitation (LARP), and colloidal synthesis, which allow control over nanoparticle size, surface chemistry, and charge transport characteristics [25–27]. By definition, QDs are nanoparticles with diameters of roughly $2-10$ nm. Their distinctive physicochemical characteristics, including a size-dependent electronic structure and adjustable surface chemistry, distinguish them from their bulk counterparts. The structural morphology of $CsPbBr_3$ exhibits a uniform distribution of QDs by transmission electron microscopy along with the desired structural planes (Fig. 1 (a)). As a result, QDs offer tunable optoelectronic properties and precise control over energy levels. Quantum confinement occurs when the size of a semiconductor nanoparticle becomes comparable to its Bohr exciton radius (Fig. 1 (b)). This leads to a transition from continuous energy states near the Fermi level to discrete, atom-like energy levels. As a result, QDs exhibit size-dependent optoelectronic properties, allowing precise control over their energy levels [6]. Fig. 1 (c) illustrates the emission wavelength ranges of commonly used QDs across the visible (VIS), near-infrared (NIR), and short-wavelength infrared (SWIR) spectral regions. Materials

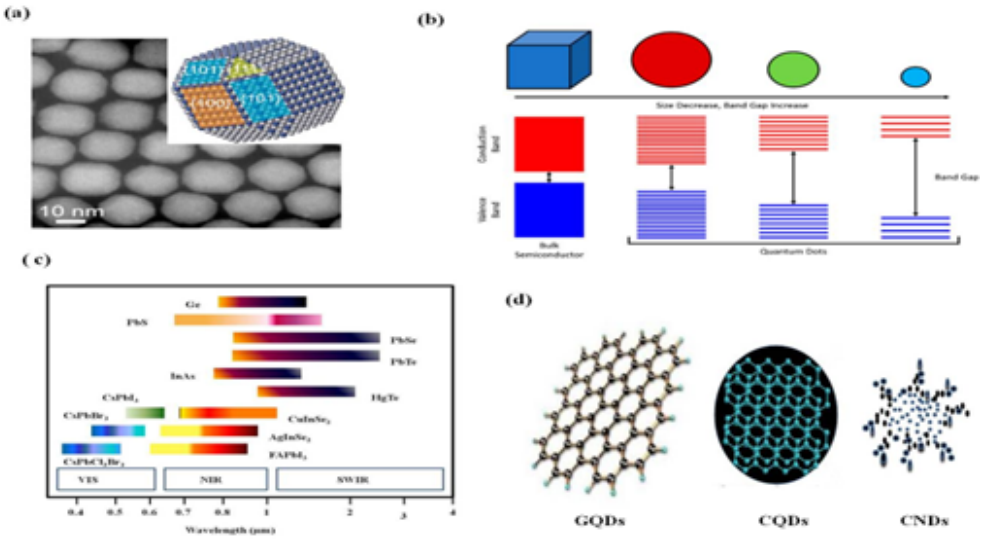

Figure 1. (a) Transmission Electron Microscopy (TEM) image of a $CsPbBr_3$ QDs and oblique packing. Reprinted with permission [6]. (b) Size-dependent quantum confinement effects in QDs. Reprinted with permission [7] (c) Emission range some prominent QDs (d) Classification of carbon QDs. Adapted with permission [8].

such as $CsPbCl_3Br_3$, $CsPbBr_3$, and $CsPbI_3$ emit primarily in the VIS to NIR range, while compounds like PbS, InAs, and Ge extend their emission into the SWIR region. Notably, semiconductors such as HgTe and PbTe demonstrate broad SWIR emission capabilities, making them suitable for advanced infrared applications. This spectrum-based visualization highlights the tunability of QDs for targeted optoelectronic applications based on desired wavelength ranges [28].

QDs can be synthesized from a diverse range of materials, and even QDs composed of the same elemental constituents may exhibit distinct physicochemical properties. As illustrated in Fig. 1 (d), carbon-based QDs are broadly categorized into graphene quantum dots (GQDs), carbon quantum dots (CQDs) and carbon nanodots (CNDs). Notably, their surface-to-volume ratio increases significantly as the size of the QDs decreases. This leads to a higher exposure of reactive surface sites, such as dangling bonds and under-coordinated atoms, which enhances their tendency to aggregate. To address this challenge, QDs are typically stabilized by surface capping with suitable ligands.

2.1 Lead halide perovskite QDs

Lead halide perovskite quantum dots (LHPQDs) are of the form ABX_3 with a cubic crystal structure. In this framework, the A-site cation (often Cs^+ or $CH_3NH_3^+$) resides at the cube corners, the B-site cation (Pb^{2+}) sits at the cube center, and halide X (I^-, Br^-, or Cl^-) occupies the face centers, as illustrated in Fig. 2 (a). Thanks to quantum confinement, LHPQDs show strong size-dependent optical behavior [29–32]. For example, a study on $CsPbI_3$ QDs synthesized at various temperatures showed a systematic redshift of the photoluminescence peak from $\sim$ 670 nm to $\sim$ 700 nm as the synthesis temperature (and hence QD size) increased [20]. This demonstrates that by controlling QD size, one can tune the emission wavelength (Fig. 2 (b)). Transmission electron microscopy (TEM) of $CsPbI_3$ QDs (Fig. 2 (c)) reveals an interplanar distance consistent with the cubic (100) plane [20, 33]. Metal-halide perovskite QDs thus offer facile bandgap tuning [34]. Furthermore, they are fully solution-processable and can potentially exceed the Shockley-Queisser efficiency limit via phenomena like multiple exciton generation and tandem architectures.

2.2 Metal chalcogenide QDs

Metal chalcogenides based on cadmium (Cd), lead (Pb), and zinc (Zn) have emerged as promising functional materials in PSC architectures, each serving distinct roles based on their optoelectronic properties and compatibility with the perovskite structure. In addition to this, several types of metal chalcogenide QDs are widely used in PSCs to enhance light absorption, charge transport, and device stability. For instance, cadmium selenide or sulfide QDs (CdSe, CdS) often serve as electron transport materials or interfacial layers due to their favorable conduction band alignment and high electron mobility [35]. Additionally, Cd-based QDs can enhance light harvesting in the visible region, despite the fact that their toxicity poses environmental concerns. Lead-based chalcogenide QDs, including PbS and PbSe, are primarily employed as co-absorbers to extend light absorption into the NIR, complementing the spectral response of the perovskite layer. Moreover, Pb-based QDs are also incorporated into quantum dot-based perovskites, enabling tunable optoelectronic properties through quantum confinement effects. Despite their effectiveness, the presence of lead compounds further contributes to toxicity issues in PSCs. In contrast, zinc-based chalcogenides, such as ZnS and ZnO offer non-toxic and stable alternative for use as ETLs, surface passivation layers, and window materials. Their wide bandgap ($\sim 3.3 - 3.6$ eV) makes them highly transparent to visible light, allowing them to act as optically transparent layers that facilitate light transmission to the underlying perovskite absorber [46]. In addition, they exhibit excellent electron mobility and interfacial compatibility, making them effective for charge extraction while also improving the thermal and environmental stability of the device. The distinct functionalities of these metal chalcogenides demonstrate their vital roles in improving efficiency, stability, and spectral utilization in perovskite solar cell technologies [47–49].

A summary of commonly used metal chalcogenide QDs, along with their key properties and roles in PSCs, is presented in Table 1.

2.3 Carbon-based QDs

Carbon-based quantum dots (CQDs), including graphene quantum dots (GQDs) and carbon nanodots (CNDs), offer an environmentally friendly alternative with unique advan-

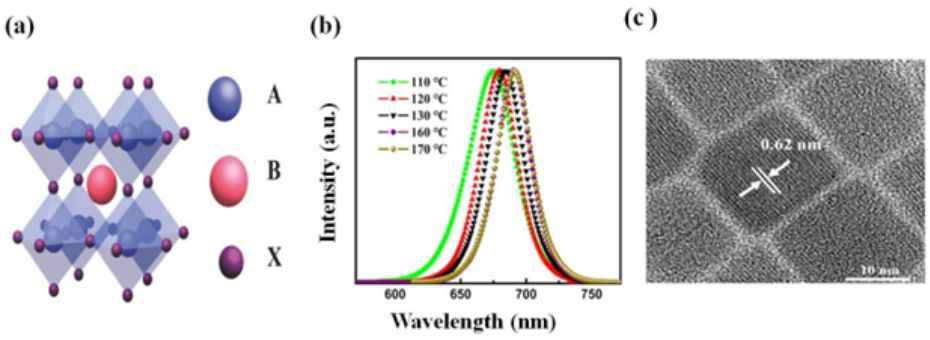

Figure 2. (a) Crystal structure of ABX_3 Perovskite QDs. (b) Normalized photoluminescence emission spectra of $CsPbI_3$ QDs synthesized at different temperature. (c) High-resolution TEM image of $CsPbI_3$ QDs, Reproduced with permission [20].

Table 1. Commonly used metal chalcogenide quantum dots in perovskite solar cells and their characteristics.

QD Material	Bandgap (eV)	Absorption Range	Role in PSCs	Toxicity Concerns	PCE (%)	Reference
CdSe	∼1.74	Visible-NIR	Light harvesting, spectral converter	Yes	∼15 – 17	[36]
PbS	∼0.41 – 1.5	NIR	Light harvesting, charge transport	Yes	∼10 – 13.8	[37]
InP	∼1.34	Visible-NIR	Light harvesting, spectral converter	Low	∼14 – 16.2	[38]
$CuInS_2$	∼1.5	Visible	Light harvesting, eco-friendly alternative	Low	∼17 – 18.6	[39]
Ag_2S	∼1.0 – 1.5	NIR	Charge transport, non-toxic QD	Low	∼11 – 13.5	[40]
CdS	∼2.42	UV-Visible	Electron transport layer, interface passivation	Yes	∼15 – 18	[15]
PbSe	∼0.27 – 1.5	NIR	Light harvesting, spectral conversion	Yes	∼10.38	[41]
ZnS	∼3.6	UV	Passivation layer, Barrier layer	Low	∼16 – 19	[42]
ZnO	∼3.3	UV	Electron transport layer	Low	∼18.67 – 19.05	[43]
$CuZnSnS_4$	∼1.4 – 1.6	Visible	Enhanced electron and hole extraction and transport	Low	∼15.4	[44]
MoS_2	∼1.8 – 1.9	UV-NIR	Enhance the electron extraction and reduced the carrier recombination	Average	∼10.02	[45]

tages [50]. They exhibit high electrical conductivity, excellent photo-stability, and strong binding interactions at the perovskite interface [51]. GQDs, owing to their high carrier mobility and crystalline structure, are utilized to improve electron transport and passivate trap states in perovskite films, leading to enhanced higher efficiency and better moisture resistance. CNDs, with their excellent dispersibility and photostability, are used as additives or buffer layers to improve film formation and reduce interfacial defects. Additionally, their intrinsic hydrophobic properties contribute significantly to moisture resistance, thereby improving the long-term environmental stability of PSCs [52]. The integration of CQDs into PSCs has demonstrated promising improvements in both power conversion efficiency and operational durability, positioning them as a compelling alternative to conventional metal-based QDs.

As illustrated in Fig. 3, CQDs enhance PSC performance by passivating trap states in the perovskite layer, reducing recombination, increasing charge transport, and providing a barrier against moisture ingress. This schematic representation highlights the multi-functional role of carbon QDs in reinforcing both the electrical and environmental stability of the device.

2.4 Si and Cu-based QDs

In recent years, emerging QDs materials such as silicon (Si) QDs and copper (Cu) QDs have attracted growing attention as environmentally friendly alternatives to traditional Pb-based QDs for integration in PSCs. Si-QDs, derived from earth-abundant elements, offering high stability, broad absorption spectra, and excellent surface passivation capabilities, making them promising candidates for enhancing the optoelectronic properties of PSCs [50–53]. Moreover, Si QDs can assist in reducing surface defects and improve charge carrier lifetime, which contributes significantly to device stability and efficiency. On the other hand, copper-based QDs (e.g. $CuInS_2$, Cu_2ZnSnS_4), have tunable bandgaps in the visible range and low toxicity; which are quite effective for photovoltaic applications [54–56]. These QDs also demonstrate strong photo stability and minimal environmental risks compared to Cd or Pb-based counterparts. Although Si- and Cu-based QDs possess promising properties, Pb-based QDs have demonstrated superior performance in photovoltaic applications. This is largely due to ongoing research on surface engineering and interface optimization, which continues to enhance their efficiency and stability.

While the above synthesis methods (e.g., hot-injection,

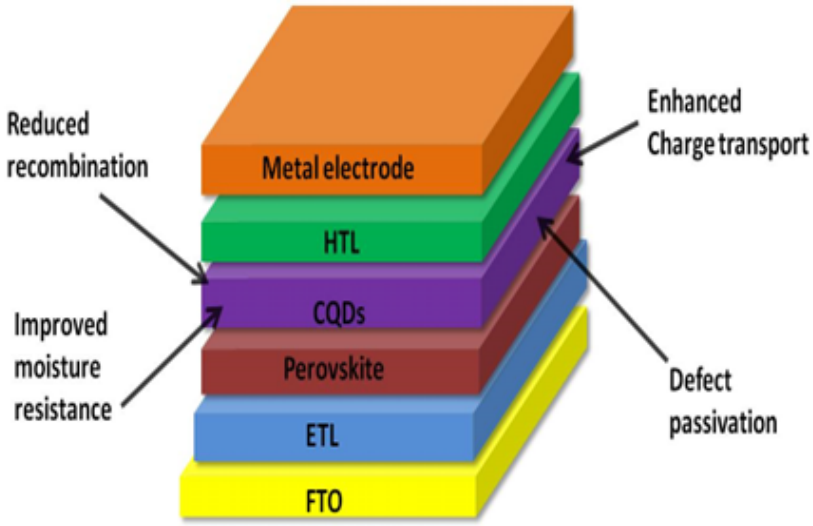

Figure 3. Schematic diagram showing how carbon-based quantum dots enhance PSC performance.

ligand-assisted reprecipitation) provide precise control over QD size and surface chemistry, their scalability and reproducibility vary considerably. For instance, the hot-injection method yields highly crystalline QDs with narrow size distributions, but it requires stringent temperature control and inert conditions, limiting large-scale production. In contrast, ligand-assisted reprecipitation and colloidal synthesis are more scalable and cost-effective, though they often suffer from broader size distributions and reduced reproducibility across batches. Continuous-flow microreactor techniques have recently emerged as a promising alternative, offering better process control and industrial scalability, but they remain underexplored in the context of PSC integration. Overall, achieving reproducible, large-scale synthesis of QDs with uniform optoelectronic properties remains a key challenge for their commercialization in perovskite solar cells.

2.5 Comparative discussion: Advantages, limitations, and unresolved issues

This review goes beyond a descriptive listing by comparing QD classes in terms of electronic properties, stability behaviour, device-level limitations, and sustainability. As summarized in Table 1, lead-halide perovskite QDs provide excellent bandgap tunability and interfacial energy-level matching, but their Pb content and phase instability remain key bottlenecks. Metal-chalcogenide QDs (Table 2) can extend absorption into the near-infrared and enhance charge extraction, yet toxicity (Pb/Cd) and surface-trap-assisted recombination require careful ligand and interface engineering. Carbon-based QDs are attractive for their low toxicity and chemical robustness, but their performance benefits can be limited by insulating surface groups and batch-to-batch variability. Finally, emerging low-toxicity QDs (Si/Cu/In-based) show promising stability benefits but still lag in reproducible high-PCE demonstrations. Across categories, unresolved issues include ligand detachment under bias/heat, QD aggregation during film formation, and long-term interfacial chemical reactions with perovskites. A comparative summary of various QD materials that contrasts the key advantages and disadvantages of each QD category is given in Table 2.

3. Photovoltaic cell characterizations

To optimize QD-PSC devices, a suite of characterization methods is employed. Standard solar-cell measurements are used to quantify how QD incorporation affects performance and elucidate the underlying mechanisms. In QD-integrated PSCs, these measurements are primarily used to elucidate improvements in charge extraction, defect passivation, recombination suppression, and operational stability, rather than to establish fundamental solar-cell theory [68, 69]. Current-Voltage (J-V) measurements under standard AM 1.5 G illumination provide key performance parameters, including open-circuit voltage (V_{OC}), short-circuit current density (J_{SC}), fill factor (FF), and power conversion efficiency (PCE). In QD-modified devices, enhanced JSC and FF are commonly observed, reflecting improved light harvesting and more efficient charge transport at QD-modified interfaces [59]. Reduced J-V hysteresis is also frequently reported, indicating suppression of interfacial charge trapping and ion migration [60, 70]. External quantum efficiency (EQE) measurements offer spectral insight into the contribution of QDs to photocurrent generation. The incorporation of QDs often leads to enhanced EQE in the ultraviolet, visible, or near-infrared regions, depending on QD composition, confirming their role in spectral broadening and improved photon utilization [71, 72]. Additional techniques such as steady-state and time-resolved photoluminescence are widely used to probe defect passivation effects, where prolonged carrier lifetimes indicate reduced non-radiative recombination [73–75]. Impedance spectroscopy further supports these findings by revealing lowered recombination resistance and improved interfacial charge transport in QD-integrated devices.

4. Strategies for photovoltaics

Over the past two decades, interface engineering has become a pivotal strategy for improving PSC performance and

Table 2. Comparative overview of quantum dot (QD) categories used in perovskite solar cells (PSCs).

QD category	Typical examples	Typical role(s) in PSCs	Key advantages	Key limitations	Representative refs.
Lead-halide perovskite QDs (PQDs)	$CsPbI_3$, $CsPbBr_3$, $FAPbI_3$ PQDs	Interfacial passivation; band alignment interlayers; spectral conversion	High PLQY; defect tolerance; energy levels compatible with perovskites; solution-processable	Pb toxicity; phase instability (α/γ); ligand insulating barriers; moisture sensitivity	[26, 27, 57, 58]
Metal chalcogenide QDs	PbS, CdSe, ZnS, MoS_2 QDs	ETL/HTL modification; broaden absorption (NIR); recombination suppression	Strong NIR absorption (PbS); tunable bandgap; can improve extraction and stability	Toxicity (Pb/Cd); surface traps; aggregation; interfacial band-mismatch if not engineered	[32, 33, 59, 60]
Carbon-based QDs	Carbon dots, graphene QDs (GQDs), N-doped CQDs	Defect passivation; hydrophobic barrier; conductivity enhancement in transport layers	Low toxicity; chemical stability; facile synthesis; good moisture resistance	Variable surface chemistry; possible insulating shells; limited NIR absorption	[42, 44, 61, 62]
Si/Cu/In-based (low-toxicity) QDs	Si QDs, $CuInS_2$, $CuInSe_2$, Cu2ZnSnS4	Lead-free passivation additives; interfacial modifiers	Low toxicity; good photostability; potential for sustainable PSCs	Lower device PCE in most reports; challenging surface control; possible deep traps	[63, 64]
QD-enabled tandem / hybrid architectures	Perovskite/PbS QD tandems; printable PQD inks	Infrared bottom sub-cell; interconnection layers; scalable printing	Spectral utilization beyond single-junction; compatibility with low-temp processing	Series resistance and recombination junction losses; stability of stacked interfaces	[65–67]

stability of PSCs. This approach primarily focuses on four key areas: band alignment strategies, surface passivation using quantum dots (QDs), ligand engineering for improve charge transfer, and Improved light absorption [76].

4.1 Band alignment strategies

Effective band alignment is essential for optimizing charge carrier dynamics in PSCs. By precisely tuning the energy levels of the constituent layers, it is possible to facilitate directional charge transport while suppressing interfacial recombination losses. A widely adopted approach involves the introduction of interlayer materials with appropriate energy levels to create a favorable energy landscape for charge extraction. The alignment of energy levels at the interfaces between the perovskite/hole transport layer (HTL) and perovskite/electron transport layer (ETL)-plays a critical role in governing efficient charge carrier extraction in PSCs. Discrepancies in energy level alignment exceeding 0.1 eV can lead to band bending at these interfaces, thereby charge transport is hindered during the formation of an energy barrier. Such misalignments not only reduce carrier extraction efficiency but also enhance interfacial recombination and promote charge accumulation. These interfacial issues have been associated with undesirable phenomena, including current-voltage hysteresis and V_{OC} deficits [77, 78]. Consequently, for optimal charge extraction and device performance, it is essential to ensure that the energy levels of both ETL and HTL are closely matched with those of the perovskite absorber layer.

QDs are promising materials to enhance energy level alignment and facilitate efficient charge carrier extraction in PSCs, for their tunable electronic structure and nanoscale dimensions. A huge range of QDs-including carbon, lead sulfide and selenide based QDs have been strategically integrated at various PSCs interfaces to improve interfacial charge dynamics [81]. For instance, Fig. 4 (a) presents schematic diagrams comparing the electron injection dynamics at the Perovskite/ETL interface for the control and GOQD-treated systems. The incorporation of GOQDs significantly reduces the electron injection time ($260-307$ ps to $90-106$ ps), indicating more efficient charge extraction. And Fig. 4 (b) presents transient absorption spectroscopy data, where normalized kinetic traces at 760 nm (photobleaching) and 530 nm (photoinduced absorption) reveal faster carrier dynamics and reduced recombination in QD-treated samples (red curves) compared to the control (black curves).

QDs can also facilitate interfacial band bending, thereby enhancing energy level alignment by minimizing energy offsets at critical junctions. For instance, adding $MAPbBr_{0.9}I_{2.1}$ QDs at the perovskite/HTL interface, resulting in the formation of a unified Fermi level between the perovskite and the QDs. This alignment significantly improves holes extraction efficiency by creating a more favorable energetic landscape for carrier transport as shown in the Fig. 4 (c) [79].

Beyond interfacial engineering, the formation of graded heterojunctions through QDs incorporation has demonstrated significant potential for enhancing charge carrier dynamics in PSCs. For instance , Zai et al. reported that anti-solvent engineering can induce the formation of a $CsPbBr_3$-rich surface layer, whose valence band is well aligned with that of the HTL, thereby facilitating more efficient hole transport, resulting in an enhanced PCE 20.56% as shown in Fig. 4 (d) [61]. Similarly, Tipparak et al. achieved comparable improvements by depositing $Cs_{1-\gamma}MA_{\gamma}PbI_{3-x}Br_x$ films at top $MAPbI_3$ layers [62]. This modification led to an up shift in the valence band position, resulting in increased hole extraction at the perovskite/HTL interface.

In addition, QDs can interact with defect states within perovskite films, effectively passivating them by narrowing band-tail electronic states and reducing the density of mid-gap states [82]. This defect passivation leads to suppressed nonradiative recombination and contributes to more favorable energy level alignment. QDs also have the potential to function directly as charge transport layer materials [94]. For example, SnO_2-QDs, have demonstrated excellent energy level compatibility with perovskite absorbers, resulting in enhanced charge transfer efficiency and reduced interfacial recombination, as summarized in Table 3.

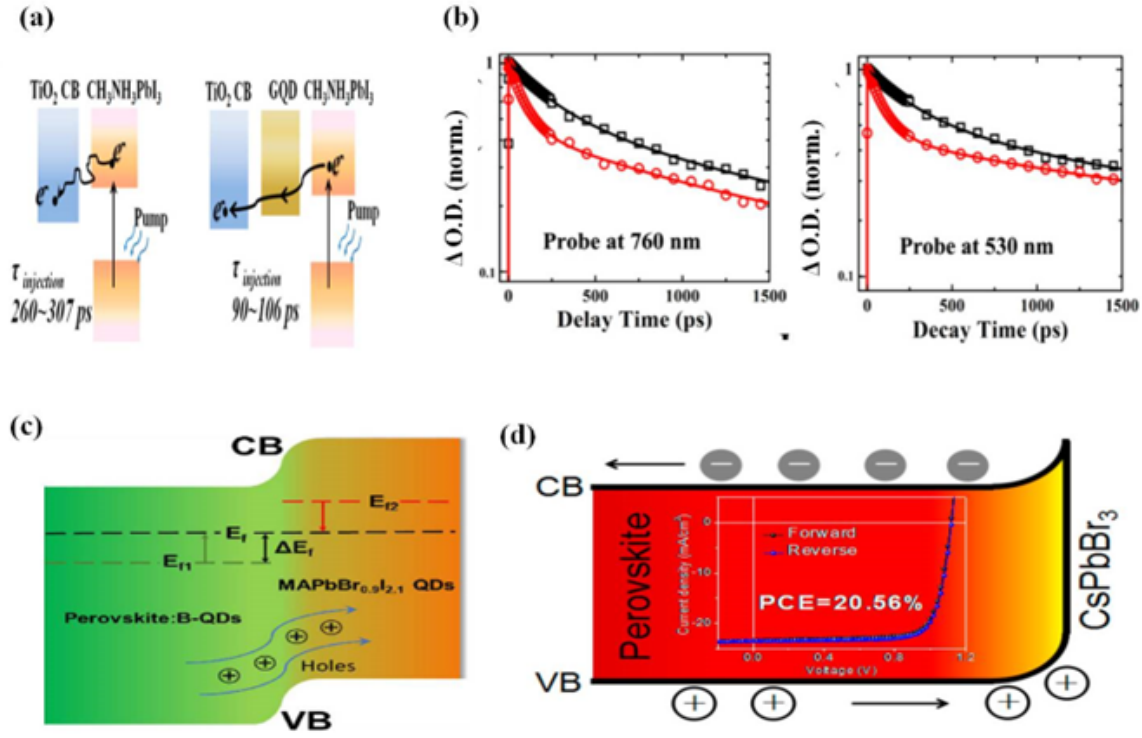

Figure 4. (a) Electron generation and extraction at the control and GO QD-treated interfaces (b) Time evolution of excited perovskite via transient absorption spectroscopy. Reproduced with permission [79]. (c) Band bending in the heterojunction structure formed between perovskite and I-QDs. Adapted with permission [80]. (d) Band alignment in a graded heterojunction structure [61].

4.2 Surface passivation with quantum dots

Surface passivation is a critical technique in PSCs aimed at mitigating non-radiative recombination by neutralizing defects at the perovskite surface and grain boundaries. These defects, often arising from under coordinated ions or vacancies, can trap charge carriers, leading to energy losses and reduced device performance. QDs are employed as passivating agents for their tunable electronic properties and high surface area. They interact with the perovskite layer through chemical bonding or electrostatic interactions, thereby passivating surface traps and enhancing charge carrier dynamics.

The mechanism involves the deposition of QDs, such as PbS, CdSe, or perovskite-based QDs like $CsPbBr_3$, onto the perovskite layer, where they form a passivation layer that reduces trap states and facilitates better energy level alignment [95]. This alignment aids in efficient charge extraction and transport, which directing to improved Voc and FF. For instance, a study demonstrated that incorporating $MAPbI_3$ QDs synthesized via a ligand-assisted reprecipitation method into CsFA perovskite solar cells resulted in enhanced performance metrics [96].The use of fluorinated graphene QDs, which not only passivate defects but also impart hydrophobicity to the perovskite layer, thereby enhancing environmental stability, which has been explored in the nearest advancements [97]. Additionally, integrating QDs as crystallization seeds has been shown to improve the quality of $FAPbI_3$ perovskite films, leading to better device performance [98]. These strategies underscore the multifaceted role of QDs in surface passivation, contributing to both the efficiency and longevity of PSCs.

In summary, the application of QDs for surface passivation in PSCs has proven to be a potent approach to address defect-related challenges. By mitigating non-radiative recombination and enhancing charge transport, QD-based passivation strategies have significantly advanced the performance and stability of PSCs, marking a pivotal step towards their commercial viability.

Table 3. Photovoltaic parameters of PSCs in energy level alignment by QDs.

Quantum Dots type	Device configuration	Optimized PCE (initial)	J_{sc} [mA/cm^2]	V_{OC} [V]	FF [%]	Ref.
CDs	FTO/c-TiO_2/CDs@m-TiO_2/$MAPbI_3$/Spiro-OMeTAD/Au	18.82 (15.60)	23.22	1.08	74.71	[83]
CDs	ITO/TiO_2/$MAPbI_3Cl_{3-x}$/Spiro-OMeTAD/Au	17.60 (12.70)	21.36	1.14	78.00	[77]
Eu–WO_x QDs	ITO/SnO_2@Eu–WO_x/$FAMAPbI_3Cl_{3-x}$/Eu–WO_x@Spiro-OMeTAD/Au	22.08 (19.03)	23.74	1.14	78.52	[84]
Au QDs	ITO/TiO_x/Perovskite/Spiro-OMeTAD/Ag	16.20 (13.02)	19.90	1.08	75.60	[85]
Au/CdS QDs	FTO/SnO_2 QDs/$(CsPbI_3)_{0.04}(FAPbI_3)_{0.82}(MAPbBr_3)_{0.14}$/Au@CdS/Spiro-OMeTAD/Au	21.39 (18.37)	23.04	1.13	81.20	[86]
Carbon QDs	ITO/CDs@SnO_2/$Cs_{0.05}FA_{0.81}MA_{0.14}PbI_{2.55}Br_{0.45}$/Spiro-OMeTAD/$MoO_3$/Au	22.77 (19.15)	24.10	1.14	83.00	[87]
GQDs	ITO/GQDs@SnO_2/$MAPbI_3$/Spiro-OMeTAD/Au	20.31 (17.91)	22.94	1.11	77.00	[88]
CdSe QDs	ITO/PEDOT:PSS/$MAPbI_{3-x}Cl_x$/CdSe QDs@PCBM/Rhodamine 101/LiF/Ag	13.73 (11.22)	20.96	0.90	73.16	[89]
CNQDs	FTO/SnO_2/g-CNQDs/Perovskite/Spiro-OMeTAD/Ag	20.23 (18.42)	23.41	1.13	76.90	[90]
$CuInS_2$ QDs	FTO/TiO_2/$CuInS_2$ QDs/$MAPbI_3$/Spiro-OMeTAD/Au	13.30 (8.20)	19.20	0.98	71.00	[91]
Mn-doped $CsPbI_3$ QDs	FTO/c-TiO_2/$CsPbI_2Br$/Mn-doped $CsPbI_3$ QDs/PTAA/Au	13.45 (12.39)	14.25	1.18	80.20	[92]
$PbSO_4(PbO)_4$ QDs	FTO/c-TiO_2/m-TiO_2/$MAPbI_3$/$PbSO_4(PbO)_4$ QDs/Spiro-OMeTAD/Au	20.02 (16.86)	24.68	1.10	75.00	[93]

4.3 Ligand engineering for improved charge transfer

Ligand engineering plays a critical role in tuning the optoelectronic properties of perovskite quantum dots (PQDs) by modifying their surface chemistry to facilitate efficient charge transfer. The primary mechanism involves tailoring the interaction between PQDs and charge-transporting layers by replacing long-chain insulating ligands with shorter or multifunctional ligands that enhance electronic coupling [68]. Traditional ligands like oleylamine (OLA) and oleic acid (OA) are effective during synthesis for colloidal stability, but their insulating nature and dynamic binding hinder charge transport by introducing barriers and trap states [99]. To address this, researchers have employed short-chain ligands such as butylamine, ethylamine and bifunctional ligands such as 3-mercaptopropionic acid and thiocyanate that offer better binding and electronic interaction with PQD surfaces [100]. Recent literature emphasizes that conductive/strong-binding ligand designs and printable QD inks are central to achieving both high efficiency and long-term stability in QD-PSCs [57, 58, 66].

These shorter or chelating ligands enable stronger coupling between QDs and improve charge delocalization, thereby promoting efficient carrier injection/extraction [101]. Bidentate ligands also contribute to better surface passivation and reduced defect density, leading to suppressed non-radiative recombination. However, this ligand exchange process must be carefully controlled, as excessive removal or replacement can compromise colloidal stability and induce PQD aggregation [102]. The advantage of ligand engineering lies in its ability to fine-tune energy levels, minimize interface losses, and improve carrier mobility; however, disadvantages include potential phase instability and ligand detachment under environmental stress.

To further improve charge transfer efficiency, strategies such as dual-ligand systems, post-synthetic surface treatment, and ligand cross-linking have been employed, yielding solar cell power conversion efficiencies exceeding 18% in some all-inorganic systems [103]. Future efforts may focus on designing ligands with tailored functionalities-such as conjugated backbones, zwitterionic groups, or self-assembling properties to achieve both strong binding and high conductivity, thus enabling scalable and stable optoelectronic devices.

4.4 Improved light absorption

QDs have emerged as powerful spectral converters in photovoltaic devices, particularly in enhancing the light-harvesting capabilities of PSCs. By absorbing high-energy photons and re-emitting them at longer wavelength, a process known as photoluminescent downshifting-QDs help align the incident light more effectively with the perovskite absorption spectrum. This spectral tuning minimizes thermalization losses that typically occur when photons with energies above the band gap are absorbed, thereby enhancing carrier generation and overall device efficiency [104, 105]. Recent advancements have demonstrated that embedding QDs such as CdSe, InP, or carbon-based QDs into perovskite layers or on top of the device can significantly boost photocurrent by broadening the absorption window and improving light harvesting under UV and visible light [106–108]. Furthermore, QDs can also reduce interfacial recombination losses and serve as passivation agents, enhancing charge separation and transport [18]. This multifaceted role of QDs in manipulating the photonic environment positions them as vital components for next-generation perovskite solar cell designs aimed at achieving higher power conversion efficiencies.

4.5 QD-perovskite interface physics

Beyond improving absorption, QDs modify the physics of the perovskite interface by creating interfacial dipoles that tune band bending, passivating under-coordinated Pb/halide defects to suppress non-radiative recombination, and changing local ion-migration pathways. However, these benefits depend strongly on QD surface chemistry: long insulating ligands can impede charge transfer, while overly aggressive ligand exchange may introduce new mid-gap states or trigger QD aggregation. Unresolved issues include the chemical stability of QD-perovskite bonding under prolonged illumination and heat, and the reproducibility of interfacial coverage at scale.

5. Device architectures and performance metrics

Over the past decades, significant advancements have been made in the design and performance of QD-integrated PSCs. These developments encompass various device architectures, including conventional and inverted structures, as well as tandem configurations, each offering unique benefits and challenges. Evaluating these architectures involve analyzing key performance metrics such as, J_{sc}, V_{OC}, FF and PCE. Additionally, establishing standardized stability testing protocols is crucial for assessing the long-term viability of these solar cells [109, 110].

5.1 Conventional vs. inverted architectures

In QD-integrated PSCs, the choice between conventional and inverted architectures significantly impacts device performance and stability. Two predominant device configurations have been adopted in PSCs: the conventional (n-i-p) architecture and the inverted (p-i-n) architecture as shown in the Fig. 5 (a) respectively. These configurations differ primarily in the sequence of layer deposition and the charge extraction pathway. In the conventional architecture, a transparent conductive oxide (TCO) (e.g. FTO) is first coated with an ETL, then the perovskite absorber, followed by a HTL, and a top metal electrode (e.g. Ag, Au). In contrast, the inverted architecture begins with the deposition of the HTL on a TCO substrate (e.g. ITO), followed by the perovskite layer, the ETL, and a top electrode.

In addition to the layer sequence, the n-i-p and p-i-n architectures differ in their interfacial energetics and hysteresis behaviour. Figure 5 (b) conceptually compares representative band diagrams, highlighting how QD interlayers can reduce interfacial barriers, increase built-in potential utilization, and suppress interfacial recombination. Hysteresis suppression is commonly attributed to reduced interfacial trap density and mitigated ion accumulation; QDs can contribute

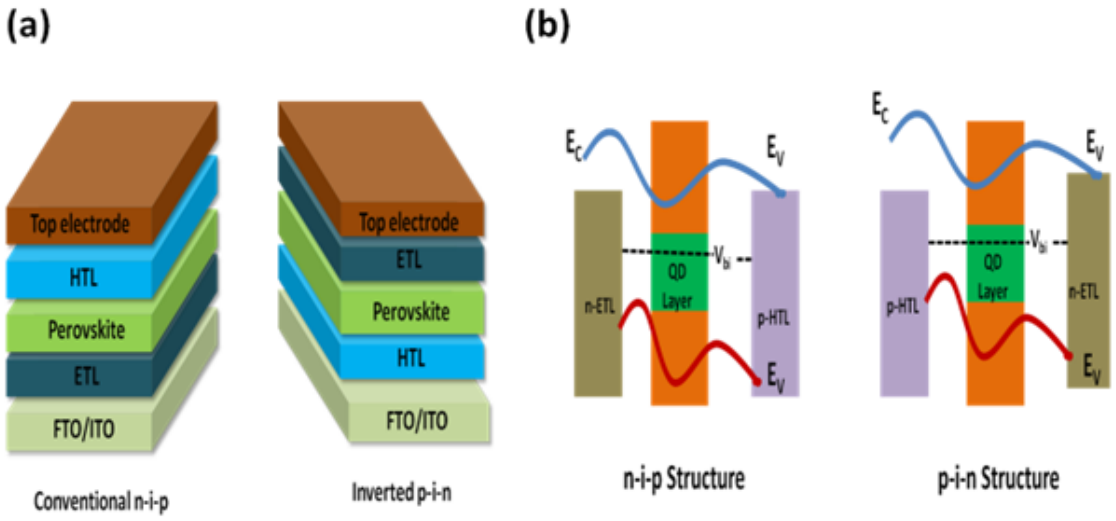

Figure 5. (a) Schematic diagrams of PSC in the Conventional n-i-p structure and inverted p-i-n structure. (b) Representative band-diagram comparison for n-i-p vs. p-i-n PSCs with a QD interlayer.

by passivating interface defects and forming ion-blocking or dipole-modifying layers. We also note that QD deposition uniformity and ligand stability are major sources of performance variability; therefore, reproducibility should be assessed using statistics over multiple devices and by reporting stabilized power output where possible. The blue and red curves denote the position of the conduction-band minimum (E_C) and valence-band maximum (E_V), respectively, across the device stack. In both architectures, the QD layer introduces intermediate energy levels that reduce abrupt band offsets at the perovskite/transport-layer interfaces, enabling more favorable "cascade" alignment for charge extraction. The built-in potential (V_{bi}), indicated by the dashed reference level and arrow, represents the internal electrostatic driving force for charge separation. By improving band alignment and passivating interfacial trap states, the QD interlayer suppresses non-radiative recombination at the contacts, thereby supporting higher V_{OC}, reduced hysteresis, and improved device stability in both n-i-p and p-i-n configurations.

5.1.1 n-i-p architecture

In conventional structures, QDs are primarily employed at the ETL/perovskite interface (e.g., TiO_2, SnO_2). QDs such as PbS, CdSe, and carbon QDs enhance electron extraction, passivate interfacial traps, and suppress recombination losses. For example, PbS quantum dots deposited on TiO_2 particularly when combined with interfacial passivation or atomic-layer-deposited (ALD) TiO_2 have been reported to enhance electron injection and collection, increase Jsc, and improve PCE; interface engineering can also suppress recombination-related hysteresis in the J–V response [111]. Similarly, red-carbon QDs incorporated into SnO_2 ETLs yielded efficiencies $> 21\%$ with enhanced stability [112]. Furthermore, QDs can mitigate photocatalytic degradation of TiO_2, extending device lifetime. In a study by Thakur et al., a planar $CH_3NH_3PbI_3$ perovskite solar cell utilizing a conventional n-i-p structure achieved a PCE of 26.11%, marking a significant improvement [43].

5.1.2 p-i-n architecture

In inverted devices, QDs are often integrated within the HTL (e.g., PEDOT:PSS, NiOx) or the ETL (e.g., ZnO, PCBM). Carbon QDs in NiOx have been shown to improved hole extraction and interfacial stability, leading to prolonged device stability with T80 lifetimes exceeding 1000 hours [113]. Likewise, ZnO QDs as low-temperature ETLs have enabled flexible, low-hysteresis devices [114]. Recently, Li et al. introduced a ferrocenyl-perovskite interface layer that interacts with the perovskite and achieved PCEs up to 26.08% (small cells) and 24.51% (1.02 cm^2 cells) [115]. Each of the architecture has its own advantages. The conventional structure typically achieves higher power conversion efficiencies due to the mature optimization of its layer materials and interfaces. However, it often requires high-temperature processing steps (e.g., TiO_2 annealing), limiting its use in flexible or temperature-sensitive applications. The inverted structure, by contrast, supports low-temperature processing, making it more suitable for flexible, lightweight, and wearable solar cells, though historically it has demonstrated slightly lower efficiencies. With the strategic integration of QDs, both configurations can be engineered for enhanced performance and long-term stability. The choice between conventional and inverted architectures thus depends on the intended application, fabrication constraints, and desired stability-performance balance.

5.2 Tandem solar cells involving QDs

Tandem solar cells (TSCs) stack multiple absorbers with different bandgaps to harvest a broader spectrum and exceed the single-junction Shockley- Queisser limit. Unlike conventional solar cells that utilize only a specific portion of the solar spectrum due to their fixed bandgap, tandem solar cells employ multiple absorber layers with different bandgaps, stacked in series or parallel, to harvest a broader range of photons. Typically, high-energy photons are absorbed by the wide-bandgap top cell, while low-energy photons are captured by a narrow-bandgap bottom cell. This spectral

splitting enables tandem cells to reduce both thermalization and transmission losses, effectively increasing their PCE beyond the Shockley- Queisser limit ($\sim$ 33%) for Tandem Solar Cells.

QDs, owing to their size-dependent bandgap tunability, strong absorption coefficients, and solution- processability, are considered as a suitable material for incorporation into tandem solar architectures. The integration of QDs into tandem solar cells can occur in various configurations. A notable example is the monolithic (two-terminal) tandem solar cell structure, where a perovskite top cell is integrated with a PbS quantum dot bottom cell [65]. The design facilitates efficient absorption of the solar spectrum, with the perovskite layer capturing high-energy photons and the PbS QD layer absorbing lower-energy photons. The architecture includes layers such as ZnO nanowires passivated by SnO_2, which serve as electron transport layers, enhancing charge extraction and overall device performance. In monolithic perovskite/QD tandems, low-bandgap PbS QDs are particularly attractive as infrared bottom absorbers, while thin QD interlayers can also improve the recombination junction by tuning band alignment and passivating interface defects [67].

Theoretical models suggest that such TSCs can achieve PCEs approaching 19% under standard AM1.5G illumination, considering factors such as inter-sub cell radiative coupling [132]. Initial experimental demonstrations have shown evidence of voltage addition in these tandem structures, indicating their potential for high-performance photovoltaic applications [133]. Additionally, Tavakoli et al. developed monolithic (two-terminal) perovskite/PbS QD tandem solar cells with a PCE of 22.15% [65], underscoring the strategic role of QDs in extending the infrared response of tandem devices. In such tandems, a low-bandgap QD layer (PbS QDs in this case) serves as an efficient bottom sub-cell, harvesting the near-IR photons that the perovskite top cell cannot absorb and thereby boosting the overall current. QDs also aid the interconnection between sub-cells: by tailoring the QD's energy levels, they facilitate better band alignment at the perovskite/quantum dot interface, reducing voltage losses at the recombination junction. Recent advancements in QD-assisted tandem solar cells have indeed demonstrated remarkable improvements in both efficiency and stability. For instance, Liu et al. reported a perovskite-perovskite-silicon triple-junction cell reaching 27.1% PCE [116], and Ugur et al. achieved 33.7% with a perovskite–silicon tandem [134]; notably, both designs benefited from interface engineering concepts similar to QD integration. Moreover, QDs can improve tandem stability: a thin QD interlayer can act as a barrier to thermal and chemical degradation between stacked sub-cells. In one study, incorporating QDs in a perovskite–PbS tandem reduced the PCE loss to $\sim$6% after 500 hours (unencapsulated), compared to much higher degradation in a QD-free tandem [135]. As shown in Fig. 6, the inclusion of QD-based layers is contributing to the steady rise in tandem efficiencies, illustrating that QDs are becoming an integral component of high-performance multi-junction PSC architecture.

6. Fabrication techniques for QD-integrated PSCs

The integration of QDs into PSCs requires precise fabrication techniques to ensure uniform dispersion, optimal interface compatibility, and minimal defect formation. A numerous deposition methods have been explored, each with its advantages and limitations. This section discusses key fabrication techniques for QD-integrated PSCs, including spin-coating, atomic layer deposition, layer-by-layer self-assembly, and advanced hybrid strategies [136].

6.1 Spin-coating deposition

Spin-coating is one of the most prevalent methods for incorporating QDs into PSCs owing its simplicity, reproducibility, and cost-effectiveness. In this technique, a QD solution is dropped onto a rotating substrate, where centrifugal forces enable the uniform spreading of the material across the surface as shown in Fig. 7. The high rotation speed and airflow cause rapid solvent evaporation, yielding a smooth, thin

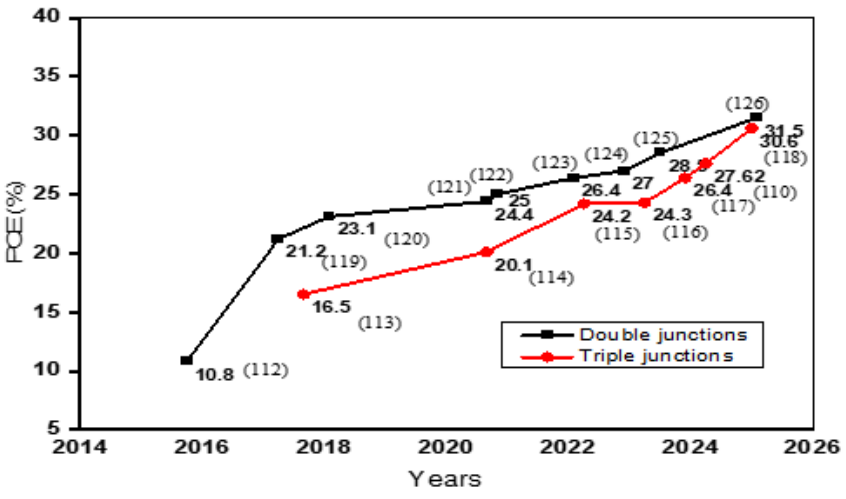

Figure 6. This graph shows the progress in PCE of double and triple-junction TSCs over the years, with corresponding reference numbers indicated in brackets- [116–131].

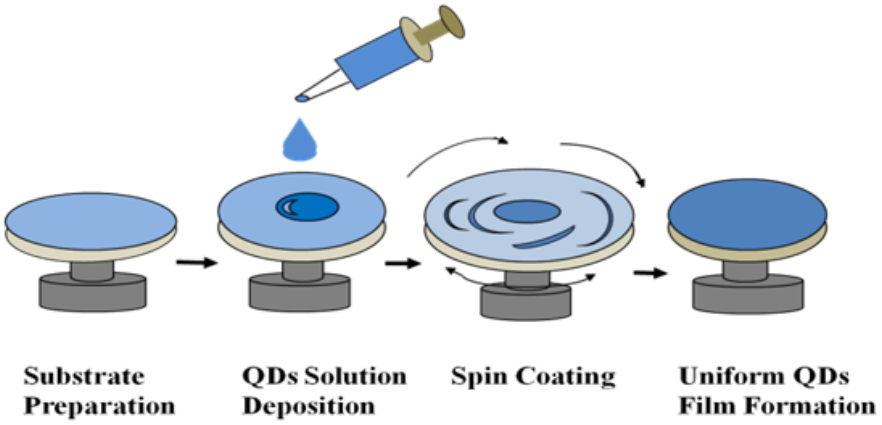

Figure 7. A schematic representation of the spin-coating process used for QD deposition in PSCs, highlighting the key steps from droplet placement to uniform film formation.

QDs film. Spin coating allows precise control over film thickness by adjusting spin speed, solution concentration and viscosity. The resultant QD films are highly sensitive to spin speed and ambient conditions like temperature and humidity. Typical spin parameters reported for QD layers are $\sim 2000-4000$ rpm for $20-40$ s, using QD dispersions in orthogonal solvents such as toluene or chlorobenzene to minimize perovskite dissolution. A frequent practical limitation is ligand exchange: incomplete replacement of long-chain ligands can reduce film conductivity, whereas overly aggressive exchange can trigger aggregation and poor coverage. The thickness of a QD layer, h, deposited by spin coating can be calculated by the following equation [137]:

$$h = \left(1 - \frac{\rho_A}{\rho_{A0}}\right)\left(\frac{3nm}{2\rho_{A0}\omega^2}\right)^{\frac{1}{3}}$$

where, ρ_A, ρ_{A0}, n, m and ω are the density of volatile liquid, initial density of the volatile liquid at the onset of spin off, viscosity of the QD solution, rate of evaporation, and angular speed of rotation respectively. The thickness and uniformity of the resulting QD film are influenced by several parameters, including spin speed, solution concentration, solvent properties, and drying conditions.

Despite its advantages, spin-coating presents challenges, particularly solvent-induced degradation of the underlying perovskite layer and inconsistent QD dispersion. The choice of solvent is critical-certain solvents can compromise the structural and chemical integrity of the perovskite layer. Yu et al. demonstrated that the solvent used during spin-coating has a substantial impact on the morphology and performance of perovskite films, underscoring the need for careful solvent engineering [138]. In addition, ligand detachment during drying or subsequent annealing can cause QD coalescence, leaving pinholes and incomplete interfacial coverage.

Another common issue is the non-uniform dispersion of QDs, often caused by the rapid solvent evaporation during spin-coating, which can kinetically trap particles and disrupt film formation. Chou et al., highlighted that final film morphology is heavily determined in the last seconds of the coating process, pointing to the importance of controlling drying kinetics through atmosphere and solvent selection [139].

To overcome these issues, several strategies have been explored. For example, incorporating additives such as amide-functionalized graphene quantum dots (AGQDs) into anti-solvents has shown improved film quality and device performance [140]. Moreover, optimizing ligand exchange processes is crucial, as the nature and concentration of ligands directly affect film formation, passivation of trap states, and charge transport port properties.

6.2 Atomic layer deposition (ALD)

Atomic layer deposition (ALD) offers precise thickness and composition control for ultra thin QDs layers in perovskite solar cells (PSCs), leading to uniform and defect-free layers that significantly enhance device performance and stability. ALD's precise deposition capabilities are instrumental in passivating defects and optimizing interfacial properties, thereby improving charge extraction and minimizing recombination losses [141].

A major challenge with traditional ALD processes is the high deposition temperatures, which can compromise the structural integrity of temperature-sensitive perovskite materials. To address this, researchers have developed low-temperature ALD techniques. For instance, Shin et. al., demonstrated the deposition of metal oxide layers at reduced temperatures, effectively preserving the perovskite structure while enhancing device stability [142]. Similarly, Zardetto et. al., reported that low-temperature ALD processes could produce high-quality oxide films without degrading the underlying perovskite layer [143].The choice of metal oxide materials deposited via ALD also plays a pivotal role in device performance. TiO_2 and Al_2O_3 are commonly used as electron transport and passivation layers, respectively. Studies have shown that incorporating these oxides can lead to significant improvements in power conversion efficiency and operational stability. For example, the integration of $TiO_2$and Al_2O_3 layers has been associated with enhanced moisture resistance and prolonged device lifetimes [144]. In practice, low-temperature ALD windows ($\sim 80-120$ °C) and carefully selected oxidants (e.g., milder H_2O vs. aggressive O_3/plasma) are used to avoid perovskite degradation, but may trade off film density and passivation

quality.
Furthermore, optimizing ALD process parameters, such as precursor selection and deposition cycles, is essential for achieving desired film properties. Advances in ALD technology have enabled the deposition of conformal and pinhole-free films at low temperatures, which are critical for the long-term stability of PSCs. These developments underscore ALD's potential in advancing perovskite solar technology by facilitating precise interface engineering and robust encapsulation strategies [145]. Precursor chemistry (e.g., TMA/H_2O for Al_2O_3 or metal-amide routes) can influence interfacial reactions and residue formation; therefore, precursor selection and purge times are critical for preventing interfacial damage and ensuring conformal coverage on rough perovskite/QD surfaces.

6.3 Layer-by-layer (LbL) self-assembly

The layer-by-layer (LbL) self-assembly technique has been extensively utilized for the deposition of QDs in photovoltaic devices. This method involves the sequential adsorption of oppositely charged species, allowing for precise control over film thickness, composition, and morphology .Such meticulous control enhances charge transport properties and device stability [142].
A significant advantage of LbL self-assembly is its facilitation of bandgap engineering through the integration of multiple QD types. For instance, the incorporation of different QDs enables the creation of graded heterojunctions, broadening the absorption spectrum and improving light-harvesting efficiency [146]. Additionally, LbL assembly has been employed to construct energy down-shifting layers on crystalline silicon solar cells, enhancing light absorption and overall device performance [147].
Despite its promising attributes, LbL self-assembly presents challenges, including extensive processing time and the necessity for precise tuning of deposition parameters to prevent film defects. Achieving uniform and defect-free films requires careful optimization of factors such as pH, ionic strength, and the molecular weight of the polyelectrolytes used [148]. Moreover, ensuring strong interfacial interactions between layers is crucial for effective charge transfer and overall device efficiency.
In LbL QD assembly, adsorption and film quality are governed by electrostatic interactions; therefore, careful control of pH (which determines the surface charge of QDs/polyelectrolytes) and ionic strength (which screens charges and alters the Debye length) is required to avoid charge neutralization and QD aggregation during sequential deposition. In practice, each adsorption step is typically followed by thorough rinsing to remove weakly bound species and a controlled drying step; otherwise, non-uniform coverage, island growth, and increased series resistance can occur. These requirements make LbL highly tunable but also sensitive to small variations in solution chemistry and processing time.

6.4 Inkjet printing and spray coating

Inkjet printing and spray coating are scalable, solution-based method suitable for depositing QDs in photovoltaic devices, including perovskite solar cells (PSCs). These methods offer rapid, large-area fabrication with minimal material waste, making them promising for industrial applications [149, 150]. For inkjet printing, reliable patterning requires a stable QD dispersion with appropriate viscosity and surface tension for jetting; overly concentrated inks or incomplete ligand exchange can cause nozzle clogging and coffee-ring drying that produces thickness non-uniformity. In addition, solvent orthogonality is crucial: the carrier solvent for QD inks should not dissolve or swell the underlying perovskite/transport layers, otherwise interfacial damage and performance scatter increase.
Inkjet printing enables precise patterning of QD layers, facilitating the fabrication of complex device architectures such as tandem and multi-junction PSCs. The high resolution of inkjet printing allows controlled layer morphology, which are essential for efficient charge transport and enhanced device performance [151]. In addition, it has the unique advantage of high resolution, low-cost, and mask-less patterning. However, challenges such as ink formulation, solvent compatibility, and printing resolution must be addressed to prevent issues like QD agglomeration and ensure uniform film formation [152].
Spray coating offers efficient deposition over large and flexible substrates, making it suitable for roll-to-roll manufacturing processes. This method has been successfully employed to fabricate various layers in PSCs, including electron transport layers and perovskite absorbers, demonstrating its versatility [153]. The spray-coating process generally comprises four sequential stages: (i) droplet generation, (ii) transport of the droplets to the substrate, (iii) coalescence of droplets into a continuous wet film, and (iv) drying of the thin film. In the context of colloidal quantum dot (CQD) deposition, a ligand-stabilized quantum dot solution is first atomized into micron-sized droplets via an orifice or ultrasonic mechanism. These droplets are then conveyed onto the substrate using a carrier gas, facilitating surface wetting [154]. Upon formation of a uniform wet film, the spray nozzle is retracted, allowing the solvent to evaporate and leaving behind a solid quantum dot layer. The successful coalescence of droplets into a film is critically influenced by several factors, including the surface tension of the ink, substrate characteristics, colloidal solution concentration, droplet size and velocity, and fluid viscosity. Furthermore, parameters such as QD solution concentration, solvent properties, substrate temperature, spray-head distance and movement speed, and fluid flow rate must be carefully optimized to mitigate issues like pooling or dewetting during solvent evaporation. The thickness achieved in a single spray pass is primarily governed by the QD concentration and duration of spraying, whereas the final film thickness is determined by the total number of spray cycles applied. Despite its advantages, spray coating faces challenges related to film uniformity, thickness control, and material utilization efficiency. Optimizing process parameters such solution concentration and substrate temperature is crucial to achieving high-quality films [155]. For spray coating, uniform coverage over large areas is limited by droplet size distribution, wetting/flow on the substrate, and solvent evaporation rate; insufficient coalescence can leave pinholes, whereas overly slow drying can induce pooling

and QD phase segregation. Managing these trade-offs (often via substrate heating, carrier-gas flow, and multi-pass deposition) is essential to prevent incomplete coverage and device-to-device variability at scale.

Both inkjet printing and spray coating hold significant potential for the scalable production of high-performance PSCs. Ongoing research focuses on addressing existing challenges, including improving ink formulations, enhancing printing resolution, and optimizing deposition parameters to achieve uniform, defect-free films. Advancements in these areas are expected to contribute to the commercialization of PSC technology.

6.5 Vapors-assisted and vacuum deposition techniques

Vapor-phase deposition techniques such as thermal evaporation and chemical vapor deposition (CVD) have also been explored for integrating quantum dots (QDs) into PSCs. These methods offer precise control over film thickness and composition, leading to superior film uniformity and enhanced interface quality, which are critical for efficient charge transport and device performance [156].

Thermal evaporation, a solvent-free process, has been successfully employed to deposit perovskite layers, minimizing solvent-related degradation and thereby enhancing the stability of PSCs [157]. For instance, researchers have utilized thermal evaporation to fabricate all-inorganic cesium-lead iodide ($CsPbI_3$) perovskite solar cells, achieving a power conversion efficiency (PCE) of 15% [158]. This approach not only improves device performance but also offers environmental benefits by eliminating the use of toxic solvents.

Chemical vapor deposition (CVD) has also been investigated for perovskite film formation. This technique enables the deposition of high-quality perovskite films with excellent uniformity and coverage, which are essential for the reproducibility and scalability of PSCs [159]. However, challenges such as high equipment costs and complex processing steps have limited the widespread adoption of CVD in perovskite solar cell fabrication.

To address these limitations, recent advancements have focused on developing low-temperature vapor-phase processes that are more compatible with perovskite materials. For example, researchers have explored hybrid deposition methods that combine vapor and solution processes to fabricate mixed-halide perovskite solar cells, aiming to enhance efficiency and stability while reducing processing complexity [160]. Additionally, efforts have been made to optimize deposition parameters to achieve high-quality perovskite films at lower temperatures, thereby preserving the structural integrity of the perovskite material and improving device longevity.

6.6 Hybrid fabrication approaches

Hybrid fabrication approaches have been developed to integrate quantum dots (QDs) into perovskite solar cells (PSCs), aiming to combine the advantages of multiple deposition techniques for enhanced performance and scalability. These methods address the limitations inherent in individual deposition processes by leveraging their complementary strengths.One notable hybrid strategy involves combining thermal evaporation with inkjet printing. In this approach, a lead iodide (PbI_2) layer is first deposited through thermal evaporation, accompanied by inkjet printing of organic cation precursors. This method also enables precise control over film thickness and composition, leading to uniform perovskite layers with improved crystallinity and coverage. Chen et al., demonstrated that optimizing the printing parameters and introducing a dimethylsulfoxide (DMSO) vapor treatment enhanced the interaction between the evaporated PbI_2 and the printed organic cations, resulting in PSCs achieving power conversion efficiencies (PCEs) up to 18.43% [161].

Another hybrid technique combines physical vapor deposition (PVD) with blade coating. Siegrist et. al., reported a fully scalable process where a triple-cation perovskite layer was formed by co-evaporating inorganic components followed by blade coating of organic cations using green solvents [162]. This approach yielded PSCs with PCEs of 18.7% on 5 cm $\times$ 5 cm substrates, highlighting the potential for large-area fabrication.

Inkjet printing has also been integrated with vapor deposition methods to enhance QD distribution and interface quality. Wilk et al., developed a process where quasi-2D perovskite layers were inkjet-printed with an optimized drying protocol, achieving PCEs of 13% for rigid and 10.6% for flexible devices [163]. This method underscores the potential of inkjet printing for scalable and flexible PSC fabrication.

Furthermore, Tan et al., employed drop-on-demand inkjet printing for quantitative surface passivation of perovskite layers [164]. By precisely controlling the deposition of passivation materials, they achieved PSCs with a high efficiency of 24.57% and improved operational stability, demonstrating the effectiveness of hybrid approaches in enhancing device performance.

7. Scalability and commercialization

For commercial viability, PSC manufacturing must transition from small-lab scales (spin-coating on 0.1 cm^2) to large-area, high-throughput processes. Techniques like spin-coating and evaporation, while offering high control, lack throughput for scaling [165]. Therefore, roll-to-roll (R2R) processing, blade coating, inject printing and spray coating are being pursued to achieve uniform, large-area modules with minimal waste [166]. Inkjet printing, for instance, enables precise deposition of QDs and perovskite layers, supporting patterned architectures for tandem devices. However, maintaining film uniformity, QD dispersion, and interfacial compatibility remains challenging at scale. Furthermore, the adaptation of QD inks to these methods often requires careful optimization of solvent systems and ligand chemistry to ensure compatibility and performance [137]. Hybrid fabrication approaches that combine scalable deposition methods with post-treatment steps such as annealing or atomic layer deposition (ALD) are also gaining traction. Advancements in these scalable strategies are vital to bridging the gap between laboratory innovation and industrial application in next-generation photovoltaics.

Translating QD-integrated PSCs from lab-scale research to industrial-scale production poses significant engineering

and economic challenges. Most high-performance QD-PSCs are fabricated using small-area spin-coating or vacuum deposition methods, which are difficult to scale up [167]. To enable commercial viability, scalable fabrication techniques that maintain device uniformity and reproducibility must be developed.

One promising approach is roll-to-roll (R2R) printing, which enables high-throughput, large-area module production with minimal material waste. R2R processing can be adapted for QD deposition, but challenges such as solvent compatibility, QD aggregation, and film uniformity must be addressed. Inkjet printing and spray coating also offer potential scalability, though QD ink formulations and deposition parameters still require optimization [168].

Achieving uniform QD dispersion without phase separation or aggregation is critical for maintaining consistent device performance across large-area modules. Researchers are exploring surfactant-assisted processing and ligand-exchange strategies to enhance QD compatibility with scalable techniques.

Finally, economic factors play a crucial role. Although perovskite materials are cost-effective compared to silicon, the expense of high-purity QD synthesis can be a limiting factor. Advances in low-cost, green synthesis methods-such as bio-inspired and solvent-free processes-could reduce production costs and enhance economic feasibility [169].

8. Stability and degradation mechanisms

Despite impressive gains in efficiency, QD-integrated PSCs under real-world conditions remains a major challenge. Perovskite materials are inherently sensitive to environmental factors such as moisture, heat, oxygen, and ultraviolet (UV) radiation, leading to degradation over time [101]. The presence of QDs within PSCs can either improve or worsen stability, depending on their composition, surface chemistry, and integration approach.

One of the primary degradation mechanisms in QD-PSCs is ion migration, where mobile halide ions move within the perovskite lattice, resulting in phase segregation and device instability [170]. Additionally, QDs themselves can suffer from ligand detachment and oxidation, further contributing to performance loss [171]. To counteract these issues, researchers have explored advanced encapsulation techniques, such as hydrophobic polymer coatings, to shield PSCs from external stressors. In situ QD formation strategies, where QDs are synthesized directly within the perovskite matrix, have also shown promise [172]. Furthermore, ligand engineering approaches such as the use of bifunctional ligands can enhance the binding stability between QDs and perovskite layers, mitigating degradation pathways.

Quantitative studies confirm that QD incorporation can extend device lifetime. For instance, Salim et al. showed that embedding PbS QDs into $FAPbI_3$ increased unencapsulated device stability from a T_{80} of $\sim$ 21 days (in N_2-fabricated controls) to $\sim$ 112 days under ambient fabrication, and up to $\sim$ 145 days with QD additives [173]. Similarly, PbS QDs passivated with a triple-cation shell retained $\sim$ 96% of their initial efficiency after 1,200 h of shelf storage [174]. In another example, perovskite-PbS QD tandem cells exhibited only $\sim$ 6% loss in PCE after 500 h of continuous illumination in ambient conditions [135]. Core-shell strategies, such as ZnS-coated Yb^{3+}-doped perovskite QDs, have further demonstrated enhanced resistance against ligand loss and oxidation, contributing to prolonged operational stability [175]. While these results are promising, most QD-PSC studies report storage or ambient-stability metrics rather than rigorous operational testing under combined light, heat, and humidity stress. In contrast, state-of-the-art non-QD PSCs can achieve T_{80} lifetimes exceeding 1,000 h under continuous illumination at 85 °C [176]. Thus, although QD integration improves relative stability, achieving the IEC 61215 commercial benchmark ($T_{80} > 5,000$ h under damp heat and thermal cycling) remains a critical challenge.

While significant progress has been made in improving the efficiency of QD-integrated PSCs, ensuring their long-term stability remains a paramount challenge. Standardized stability testing protocols are essential for reliably assessing device longevity and performance under real-world conditions [172]. Key factors influencing stability include moisture ingress, thermal stress, and photodegradation. Implementing encapsulation techniques, such as the deposition of luminescent and anti-reflective silica layers, has been shown to enhance stability by protecting the active layers from environmental factors [177]. Additionally, the use of robust transport layers and careful selection of QD surface ligands can mitigate degradation pathways [101]. Collaborative efforts among researchers, industry stakeholders, and standardization bodies are necessary to develop comprehensive guidelines that ensure the reliability and durability of these emerging photovoltaic technologies. Recent strategies increasingly combine QD passivation with 2D/3D interfacial engineering and ligand-tailored QDs to achieve higher operational stability, motivating deeper mechanistic studies and standard test protocols [57, 58, 178].

9. Toxicity concerns

A major drawback of QD-based PSCs is the environmental and health concerns associated with lead-containing perovskite materials. Most high-performance perovskite QDs, such as $CsPbX_3$ (X = Cl, Br, I), rely on lead-based compositions, which pose potential risks due to lead toxicity [32]. The leaching of lead from degraded PSCs into the environment raises concerns regarding their large-scale deployment.

To address these issues, researchers have been actively investigating lead-free alternatives, including Sn, Bi-based perovskite QDs. Tin halide perovskite QDs ($CsSnX_3$) exhibit promising optoelectronic properties, but their stability remains a significant challenge due to the high susceptibility of Sn^{2+} to oxidation [179]. Bismuth-based QDs, such as $Cs_3Bi_2X_9$, offer improved stability and reduced toxicity but generally suffer from lower efficiency [179].

Beyond perovskite-based QDs, other non-toxic materials, such as carbon-based QDs, silicon QDs, and copper indium sulfide ($CuInS_2$) QDs, have been explored [63, 64]. Carbon quantum dots, in particular, have demonstrated excellent defect passivation capabilities without introducing toxic elements. However, further research is needed to improve their

tunability and compatibility with perovskite systems.
Toxicity-performance trade-off: At present, the highest-efficiency QD-assisted PSC demonstrations most often rely on Pb-containing QDs (either perovskite QDs or PbS), whereas lead-free QDs (e.g., carbon dots, Si QDs, $CuInS_2$) generally deliver smaller efficiency gains but offer a clearer path to environmental compliance. Accordingly, future progress should couple (i) performance-oriented surface/ligand engineering with (ii) toxicity mitigation strategies such as robust encapsulation, recycling, and the accelerated development of high-electronic-quality lead-free QDs.
Regulatory frameworks and environmental policies will also play a crucial role in determining the commercial viability of QD-enhanced PSCs. Developing efficient lead-recycling strategies and encapsulation techniques to prevent lead leakage will be essential for addressing toxicity concerns.

10. Future outlook for QDs-PSC integration:

(i) Materials: Develop high-electronic-quality, low-toxicity QDs (e.g., lead-free perovskite-inspired QDs, Si/Cu/In-based QDs) and robust core-shell designs that suppress ion migration and environmental degradation.

(ii) **Surface/ligand chemistry:** Replace long insulating ligands with conductive, strongly binding ligands and cross-linkable systems to prevent ligand detachment and aggregation while maintaining charge transport; recent ligand-engineering reviews and printable QD ink reports provide a practical roadmap [57, 58, 66].

(iii) Interfaces and physics: Establish design rules for QD-induced dipoles, band bending, and defect passivation at specific PSC interfaces (ETL/perovskite, perovskite/HTL), including standardized stability tests that decouple chemical degradation from ion-migration-driven hysteresis.

(iv) Leverage QDs in tandem PSCs as infrared absorbers and interconnection modifiers to increase spectral utilization and stability, while minimizing recombination-junction losses.

(v) Scale-up: Transition from spin-coated lab devices to scalable deposition (inkjet/spray/slot-die) with statistical reporting of device-to-device variability and stabilized power output to demonstrate reproducibility.

11. Conclusion

The present study provides a detailed view of the integration of QDs into PSCs which has emerged as a transformative approach for enhancing light harvesting, improving charge carrier dynamics, and significantly boosting device stability and efficiency. One of the most significant power conversion efficiency of 33.7% is seen when QDs-Tandem solar cells architecture is employed. Diverse classes of QDs have demonstrably improved PSC efficiency and stability by passivating defects, tuning band alignment, and broadening light absorption. By leveraging these advantages, QD-enhanced PSCs are advancing toward next-generation photovoltaic performance. In particular, the advancement of hybrid and vapor-assisted fabrication methods has enabled more precise QD integration and better interface quality, offering a promising pathway toward scalable and efficient QD-PSC manufacturing. Despite of this advancement, several challenges remain, particularly concerning the toxicity of lead-based QDs, the scalability of fabrication techniques, and the long-term operational stability of QD-PSCs under real-world conditions.

Acknowledgement
The author sincerely thanks and acknowledges Science and engineering research board (SERB), Government of India for financial assistance through sanctioning core research grant (CRG/2023/006037).

Authors Contribution
Promud Konch and Prerona Singha performed data collection and their analyses, preparation of illustration for construction of review manuscript. Sagar Bhattarai involved in critical reviewing and editing. P K Kalita gave the conceptual idea for review and supervised all aspect of the manuscript.

Availability of data and materials
The data that support the findings of this study are available from the corresponding author, upon reasonable request.

Conflict of interests
The authors declare that they have no known competing financial interests or personal relationships that could have appeared to influence the work reported in this paper.

References

[1] L. Qiu, S. He, L.K. Ono, and Y. Qi. Progress of Surface Science Studies on ABX3-Based Metal Halide Perovskite Solar Cells. *Adv. Energy Mater*, **10**(13):1902726, (2020). DOI: https://doi.org/10.1002/aenm.201902726.

[2] A. Kojima, K. Teshima, Y. Shirai, and T. Miyasaka. Organometal halide perovskites as visible-light sensitizers for photovoltaic cells. *J. Am. Chem. Soc.*, **131**(17):6050–6051, (2009). DOI: https://doi.org/10.1021/ja809598r.

[3] S.D. Stranks and H.j. Snaith. Metal-halide perovskites for photovoltaic and light-emitting devices. *Nat. Nanotechnol*, **10**:391–402, (2015). DOI: https://doi.org/10.1038/nnano.2015.90.

[4] W. Niu, X. Li, S.K. Karuturi, D.W. Fam, H. Fan, S. Shrestha, L.H. Wong, and A.I.Y. Tok. Applications of atomic layer deposition in solar cells. *Nanotechnology*, **26**(6):064001, (2015). DOI: https://doi.org/10.1088/0957-4484/26/6/064001.

[5] M. Saliba, T. Matsui, J. Seo, K. Domanski, J. Baena, M. Nazeeruddin, S.M. Zakeeruddin, W. Tress, A. Abate, and M. Gratzela. Cesium-containing triple cation perovskite solar cells: improved stability, reproducibility and high efficiency. *Energy and Environmental Science*, **9**:1989–1997, (2016). DOI: https://doi.org/10.1039/C5EE03874J.

[6] T.V. Sekh, I. Cherniukh, E. Kobiyama, T.J. Sheehan, et al. All-Perovskite Multicomponent Nanocrystal Superlattices. . *ACS Nano.*, **18**(11):8423–8436, (2024). DOI: https://doi.org/10.1021/acsnano.3c13062.

[7] Kumar D. Sumanth, Kumar B. Jai, and H.M. Mahesh. Quantum Nanostructures (QDs) : An Overview. *Synth. Inorg. Nanomater. Adv. Key Technol.*, :59–88, (2018).

[8] A. Cayuela, M.L. Soriano, C. Carrillo-Carrión, and M. Valcárcel. Semiconductor and carbon-based fluorescent nanodots: the need for consistency. *Chem. Commun.*, **52**(7):1311–1326, (2016). DOI: https://doi.org/10.1039/C5CC07754K.

[9] P.V. Kamat. Quantum Dot Solar Cells: The Next Big Thing in Photovoltaics. *J. Phys. Chem. Lett.*, **4**(6):4908–918, (2013). DOI: https://doi.org/10.1021/jz400052e.

[10] S. Akin, N. Arora, S.M. Zakeeruddin, M. Grätzel, R.H. Friend, and M.I. Dar. New Strategies for Defect Passivation in High-Efficiency Perovskite Solar Cells. *Adv. Energy Mater.*, **10**(13): 21903090, (2019). DOI: https://doi.org/10.1002/aenm.201903090.

[11] S. Rakshit, P. Piatkowski, I. Mora-seró, and A. Douhal. Combining Perovskites and Quantum Dots : Synthesis, Characterization, and Applications in Solar Cells, LEDs, and Photodetectors. *Adv. Optical Mater.*, **10**(14):2102566, (22). DOI: https://doi.org/10.1002/adom.202102566.

[12] M. Chen, J. Wang, F. Yin, Z. Du, L.A. Belfiore, and J. Tang. Strategically integrating quantum dots into organic and perovskite solar cells. *J. Mater. Chem.*, **9**:4505–4527, (2021). DOI: https://doi.org/10.1039/D0TA11336K.

[13] W. Chi and S.K. Banerjee. Development of perovskite solar cells by incorporating quantum dots. *Chem. Eng. J.*, **426**(7560):131588, (2021). DOI: https://doi.org/10.1016/j.cej.2021.131588.

[14] D. Ghosh, D.K. Chaudhary, M.Y. Ali, K.K. Chauhan, et al. All-inorganic quantum dot assisted enhanced charge extraction across the interfaces of bulk organo-halide perovskites for efficient and stable pin-hole free perovskite solar cells. *Chem. Sci.*, **10**:9530–9541, (2019). DOI: https://doi.org/10.1039/C9SC01183H.

[15] M.M. Tavakoli, H.T. Dastjerdi, D. Prochowicz, P. Yadav, R. Tavakoli, M. Saliba, and Z. Fan. Highly efficient and stable inverted perovskite solar cells using down-shifting quantum dots as a light management layer and moisture-assisted film growth. *J. Mater. Chem. A*, **7**:14753–14760, (2019). DOI: https://doi.org/10.1039/C9TA03131F.

[16] T. Chiba and J. Kido. Lead halide perovskite quantum dots for light-emitting devices. *J. Mater. Chem.*, **6**:11868–11877, (2018). DOI: https://doi.org/10.1039/C8TC03561J.

[17] D. Sensitized, S. Cells, R. Kottayi, D.K. Maurya, R. Sittaramane, and S. Angaiah. Recent Developments in Metal Chalcogenides based Quantum. *ES Energy & Environment*, **18**:1–40, (2022). DOI: https://doi.org/10.30919/esee8c754.

[18] A. Kim, J.K. Dash, P. Kumar, and R. Patel. Carbon-Based Quantum Dots for Photovoltaic Devices : A Review. *ACS Appl. Electron. Mater.*, **4**(1):27–58, (2022). DOI: https://doi.org/10.1021/acsaelm.1c00783.

[19] M.J. Molaei. The optical properties and solar energy conversion applications of carbon quantum dots : A review. *Sol. Energy.*, **196**: 549–566, (2020). DOI: https://doi.org/10.1016/j.solener.2019.12.036.

[20] F. Liu, Y. Zhang, C. Ding, S. Kobayashi, T. Izuishi, et al. Highly Luminescent Phase-Stable $CsPbI_3$ Perovskite Quantum Dots Achieving Near 100% Absolute Photoluminescence Quantum Yield. *ACS Nano.*, **11**(10):10373–10383, (2017). DOI: https://doi.org/10.1021/acsnano.7b05442.

[21] T.T. Ngo, S. Masi, P.F. Mendez, M. Kazes, D. Oron, and I.M. Seró. PbS quantum dots as additives in methylammonium halide perovskite solar cells: the effect of quantum dot capping. *Nanoscale Adv.*, **1**:4109–4118, (2019). DOI: https://doi.org/10.1039/C9NA00475K.

[22] L. Fu, H. Li, L. Wang, R. Yin, B. Li, and L. Yin. Defect passivation strategies in perovskites for an enhanced photovoltaic performance. *Energy Environ. Sci.*, **13**:4017–4056, (2020). DOI: https://doi.org/10.1039/D0EE01767A.

[23] X. Zhang, Q. Wang, Z. Jin, Y. Chen, H. Liu, and J. Wang. Graphdiyne Quantum Dots for Much Improved Stability and Efficiency of Perovskite Solar Cells. *Adv. Mater. Interfaces*, **5**(2): 1701117, (2018). DOI: https://doi.org/10.1002/admi.201701117.

[24] P. Guo, H. Zhu, W. Zhao, C. Liu, et al. Interfacial Embedding of Laser-Manufactured Fluorinated Gold Clusters Enabling Stable Perovskite Solar Cells with Efficiency Over 24%. *Adv. Mater.*, **33** (36):2101590, (2021). DOI: https://doi.org/10.1002/adma.202101590.

[25] H. Wang, Q. Su, and T. Weng. Enhancing Solar Cell Efficiency through Quantum Dots and Emerging Photovoltaic Technologies. *Highlights in Science Engineering and Technology*, **12**:545–551, (2024). DOI: https://doi.org/10.54097/v201hq10.

[26] S. Zang, J. Chen, Y. Yu, Qin X., and H. Liu. Ligand-Assisted Reprecipitation of Highly Luminescent Perovskite Nanocrystals. *ACS Appl. Nano Mater.*, **8**(7):3680–3687, (2025). DOI: https://doi.org/10.1021/acsanm.5c00412.

[27] R. Gui, H. Jin, Z. Wang, and L. Tan. Recent advances in synthetic methods and applications of colloidal silver chalcogenide quantum dots. *Coord. Chem. Rev.*, **296**:91–124, (2015). DOI: https://doi.org/10.1016/j.ccr.2015.03.023.

[28] M.C. Beard. Multiple Exciton Generation in Semiconductor Quantum Dots. *J. Phys. Chem. Lett.*, **2**(11):1282–1288, (2011). DOI: https://doi.org/10.1021/jz200166y.

[29] D. Choi, H. Kim, Y. Bae, S. Lim, and T. Park. Perovskite Colloidal Quantum Dots with Tailored Properties : Synthesis Strategies and Photovoltaic Applications. *ACS Energy Lett.*, **9**(6):2633–2658, (2024). DOI: https://doi.org/10.1021/acsenergylett.4c00632.

[30] L. Protesescu, S. Yakunin, M.I. Bodnarchuk, F. Krieg, et al. Nanocrystals of Cesium Lead Halide Perovskites (CsPbX3 , X = Cl, Br, and I): Novel Optoelectronic Materials Showing Bright Emission with Wide Color Gamut. *Nano Lett.*, **15**(6):3692–3696, (2015). DOI: https://doi.org/10.1021/nl5048779.

[31] J. Shamsi, A.S. Urban, M. Imran, Trizio L., and L. Manna. Metal Halide Perovskite Nanocrystals : Synthesis , Post-Synthesis Modi fi cations , and Their Optical Properties. . *Chem. Rev.*, **119**(5): 3296–3348, (2019). DOI: https://doi.org/10.1021/acs.chemrev.8b00644.

[32] S. Ananthakumar, J. Ram, K. Sridharan, M. Babu, J.R. Kumar, and Babu S. Moorthy. Cesium lead halide (CsPbX3, X = Cl, Br, I) perovskite quantum dots-synthesis, properties, and applications : a review of their present status. *J. Photon. Energy.*, **6**(4):042001, (2016). DOI: https://doi.org/10.1117/1.JPE.6.042001.

[33] A. Swarnkar, A.R. Marshall, E.M. Sanehira, B.D. Chernomordik, et al. Quantum dot-induced phase stabilization of α-$CsPbI_3$ perovskite for high-efficiency photovoltaics. . *Science*, **354**(6308): 92–95, (2016). DOI: https://doi.org/10.1126/science.aag2700.

[34] J. Shamsi, A.S. Urban, M. Imran, L. Trizio, and L. Manna. Metal Halide Perovskite Nanocrystals: Synthesis, Post-Synthesis Modifications, and Their Optical Properties. *Chem. Rev.*, **119**(5):3296–3348, (2019). DOI: https://doi.org/10.1021/acs.chemrev.8b00644.

[35] D. Liu, J. Liu, S. Liu, C. Wang, Z. Ge, and X. Hao. Physica E : Low-dimensional Systems and Nanostructures The photovoltaic performance of CdS / CdSe quantum dots co-sensitized solar cells based on zinc titanium mixed metal oxides. *Physica E : Low-dimensional Systems and Nanostructures*, **115**:113669, (2020). DOI: https://doi.org/10.1016/j.physe.2019.113669.

[36] N. Elmi, H. Pasdar, and M. Tavakkoli. Materials Today Sustainability CdSe nanoflower as a new near infrared-activated photocatalyst for remediation of pharmaceutical wastewaters, Mater. *Today Sustain.*, **28**:100961, (2024).
DOI: https://doi.org/10.1016/j.mtsust.2024.100961.

[37] Sadovnikov S.I. and A.I. Gusev. Structure and properties of PbS films. *J. Alloys Compd.*, **573**:65–75, (2013).
DOI: https://doi.org/10.1016/j.jallcom.2013.03.290.

[38] L. Gao, Y. Cui, R.H.J. Vervuurt, Dam D. Van, Veldhoven R.P.J. Van, et al. High-Efficiency InP-Based Photocathode for Hydrogen Production by Interface Energetics Design and Photon Management. *Adv. Funct. Mater.*, **26**(5):679–686, (2016).
DOI: https://doi.org/10.1002/adfm.201503575.

[39] A.D.P. Leach and J.E. Macdonald. Optoelectronic Properties of $CuInS_2$ Nanocrystals and Their Origin. *J. Phys. Chem. Lett.*, **7**(3): 572–583, (2016).
DOI: https://doi.org/10.1021/acs.jpclett.5b02211.

[40] W. Jiang, Z. Wu, X. Yue, S. Yuan, H. Lu, and B. Liang. Photocatalytic performance of Ag 2 S under irradiation with visible and near-infrared light and its mechanism of degradation. *RSC Adv.*, **5**: 24064–24071, (2015).
DOI: https://doi.org/10.1039/C4RA15774E.

[41] Y. Liu, F. Li, G. Shi, Z. Liu, X. Lin, Y. Shi, Y. Chen, et al. PbSe Quantum Dot Solar Cells Based on Directly Synthesized Semiconductive Inks. *ACS Energy Lett.*, **5**(12):3797–3803, (2020).
DOI: https://doi.org/10.1021/acsenergylett.0c02011.

[42] M.M. Tavakoli, D. Prochowicz, P. Yadav, and R. Tavakoli. Efficient Perovskite Solar Cells Based on CdSe/ZnS Quantum Dots Electron Transporting Layer with Superior UV Stability. *Phys. Status Solidi-Rapid Res. Lett.*, **14**(6):2000062, (2020).
DOI: https://doi.org/10.1002/pssr.202000062.

[43] A. Thakur, D. Singh, and S.K. Gill. Numerical simulations of 26.11% efficient planar $CH_3NH_3PbI_3$ perovskite n-i-p solar cell. *Material Today Proceedings*, **71**:195–201, (2022).
DOI: https://doi.org/10.1016/j.matpr.2022.08.423.

[44] L.S. Khanzada, I. Levchuk, Y. Hou, H. Azimi, and A. Osvet. Effective Ligand Engineering of the Cu_2ZnSnS_4 Nanocrystal Surface for Increasing Hole Transport Efficiency in Perovskite Solar Cells. *Adv. Funct. Mater.*, **26**(45):8300–8306, (2016).
DOI: https://doi.org/10.1002/adfm.201603441.

[45] Q. Zhou, J. Du, J. Duan, Y. Wang, X. Yang, Y. Duan, and Q. Tang. Photoactivated transition metal dichalcogenides to boost electron extraction for all-inorganic tri-brominated planar perovskite solar cells. *J. Mater. Chem. A*, **8**:7784–7791, (2020).
DOI: https://doi.org/10.1039/D0TA01645D.

[46] T. Nie, Z. Fang, X. Ren, Y. Duan, and S.F. Liu. Recent Advances in Wide - Bandgap Organic - Inorganic Halide Perovskite Solar Cells and Tandem Application. *Nano-Micro Lett.*, **15**(70), (2023).
DOI: https://doi.org/10.1007/s40820-023-01040-6.

[47] J. Ye, M.M. Byranvand, C.O. Martínez, R.L.Z. Hoye, M. Saliba, and L. Polavarapu. Defect Passivation in Lead-Halide Perovskite Nanocrystals and Thin Films : Toward Efficient LEDs and Solar Cells. *Angew. Chemie.*, **133**(40):21804–21828, (2021).
DOI: https://doi.org/10.1002/ange.202102360.

[48] D. Shin, Y. Park, H. Jeong, H.V. Tran, and E. Jang. Exploring the Potential of Colloidal Quantum Dots for Near-Infrared to Short-Wavelength Infrared Applications. *Adv. Energy Mater.*, **15**(2): 2304550, (2025).
DOI: https://doi.org/10.1002/aenm.202304550.

[49] H. Lu, Z. Huang, M.S. Martinez, J.C. Johnson, J.M. Luther, and M.C. Beard. Transforming energy using quantum dots. *Energy Environ. Sci.*, **13**:1347–1376, (2020).
DOI: https://doi.org/10.1039/C9EE03930A.

[50] B. Ali, A. Jahdaly, M.F. Elsadek, B.M. Ahmed, F. Farahat, M.M. Taher, and A.M. Khalil. Outstanding Graphene Quantum Dots from Carbon Source for Biomedical and Corrosion Inhibition Applications : A Review. *Sustainability*, **13**(4):2127, (2021). URL https://www.mdpi.com/2071-1050/13/4/2127.

[51] A. Gaurav, A. Jain, and S.K. Tripathi. Review on Fluorescent Carbon / Graphene Quantum Dots : Promising Material for Energy Storage and Next-Generation Light-Emitting Diodes. *Materials*, **15** (22):7888, (2022).
DOI: https://doi.org/10.3390/ma15227888.

[52] K. Patel, D. Prochowicz, S. Akin, A. Kalam, M.M. Tavakoli, and P. Yadav. Applications of Carbon-Based Materials for Improving the Performance and Stability of Perovskite Solar Cells. *Energy Technol.*, **11**(10):2300228, (2023).
DOI: https://doi.org/10.1002/ente.202300228.

[53] A. Jana, A. Talha, A. Ahmed, V. Gopalan, S. Youngsin, H. Kim, H. Im, and R.A. Taylor. Stabilization of halide perovskites with silicon compounds for optoelectronic, catalytic, and bioimaging applications. *InfoMat.*, **6**(12):12559, (2024).
DOI: https://doi.org/10.1002/inf2.12559.

[54] R. Zhou, J. Xu, P. Luo, L. Hu, X. Pan, et al. Near-Infrared Photoactive Semiconductor Quantum Dots for Solar Cells. *Adv. Energy Mater.*, **11**(40):2101923, (2021).
DOI: https://doi.org/10.1002/aenm.202101923.

[55] N.D. Sankir, E. Aydin, E. Ugur, and M. Sankir. Non-toxic and environmentally friendly route for preparation of copper indium sulfide based thin film solar cells. *J. Alloys Compd.*, **640**:468–474, (2015).
DOI: https://doi.org/10.1016/j.jallcom.2015.04.013.

[56] M.M. Hamasha. Environmentally Friendly Synthesis of Copper Zinc Tin Sulfide (CZTS) Thin Film Solar Cells : Advancing Sustainable Photo-Energy Conversion with Low-Temperature Chemical Processing. *Materials Research*, **27**:20240282, (2024).
DOI: https://doi.org/10.1590/1980-5373-MR-2024-0282.

[57] S. Ding, M. Hao, T. Lin, Y. Bai, and L. Wang. Ligand engineering of perovskite quantum dots for efficient and stable solar cells. . *Journal of Energy Chemistry*, **69**:626–648, (2022).
DOI: https://doi.org/10.1016/j.jechem.2022.02.006.

[58] K. Huang, J. Liu, J. Yuan, W. Zhao, K. Zhao, and Z. Zhou. Perovskite-quantum dot hybrid solar cells : a multi-win strategy for high performance and stability. *Journal of Materials Chemistry A*, **11**:4487–4509, (2023).
DOI: https://doi.org/10.1039/D2TA09434G.

[59] J. Kabel, S. Sharma, A. Acharya, D. Zhang, and Y.K. Yap. Molybdenum Disulfide Quantum Dots : Properties, Synthesis, and Applications. *Journal of Carbon Research*, **7**(2):45, (10.3390/c7020045).
DOI: https://doi.org/2021.

[60] L. Najafi, B. Taheri, B. Martín-García, S. Bellani, et al. MoS_2 Quantum Dot/Graphene Hybrids for Advanced Interface Engineering of a $CH_3NH_3PbI_3$ Perovskite Solar Cell with an Efficiency of over 20%. *ACS Nano.*, **12**(11):10736–10754, (2018).
DOI: https://doi.org/10.1021/acsnano.8b05514.

[61] H. Zai, C. Zhu, H. Xie, Y. Zhao, C. Shi, Z. Chen, et al. Congeneric Incorporation of $CsPbBr_3$ Nanocrystals in a Hybrid Perovskite Heterojunction for Photovoltaic Efficiency Enhancement. *ACS Energy Lett.*, **3**(1):30–38, (2018).
DOI: https://doi.org/10.1021/acsenergylett.7b0092.

[62] P. Tipparak, W. Passatorntaschakorn, W. Khampa, W. Musikpan, et al. The Impact of $MAPbI_3$ Quantum Dots on CsFA Perovskite Solar Cells : Interface and Hole Extraction Improvement. *ACS Appl. Energy Mater.*, **8**(1):355–365, (2025).
DOI: https://doi.org/10.1021/acsaem.4c02474.

[63] M. Bidikoudi and E. Stathatos. Chalcogenides in Perovskite Solar Cells with a Carbon Electrode : State of the Art and Future Prospects. . *Nanomaterials*, **14**(22):1783, (2024).
DOI: https://doi.org/10.3390/nano14221783.

[64] Y. Cao, P. Zhu, D. Li, X. Zeng, and D. Shan. Size-Dependent and Enhanced Photovoltaic Performance of Solar Cells Based on Si Quantum Dots. *Energies*, **13**(18):4845, (2020). DOI: https://doi.org/10.3390/en13184845.

[65] M.M. Tavakoli, H.T. Dastjerdi, P. Yadav, D. Prochowicz, H. Si, and R. Tavakoli. Ambient Stable and Efficient Monolithic Tandem Perovskite / PbS Quantum Dots Solar Cells via Surface Passivation and Light Management Strategies. . *Adv. Funct. Mater.*, **31**(21): 2010623, (2021). DOI: https://doi.org/10.1002/adfm.202010623.

[66] X. Zhang, H. Huang, C. Zhao, L. Jin, et al. Conductive colloidal perovskite quantum dot inks towards fast printing of solar cells. *Nature Energy*, **9**:1378–1387, (2024). DOI: https://doi.org/10.1038/s41560-024-01608-5.

[67] M.M. Tavakoli, H.T. Dastjerdi, P. Yadav, D. Prochowicz, H. Si, and R. Tavakoli. Ambient stable and efficient monolithic tandem perovskite/PbS quantum dots solar cells via surface passivation and light management strategies. *Advanced Functional Materials*, **31**: 2010623, (2021). DOI: https://doi.org/10.1002/adfm.202010623.

[68] Y. Zhou, J. Yang, X. Luo, Y. Li, and Q. Qiu. Selection , Preparation and Application of Quantum Dots in Perovskite Solar Cells. *Int. J. Mol. Sci.*, **23**(16):9482, (2022). DOI: https://doi.org/10.3390/ijms23169482.

[69] Y. Zhou, X. Luo, J. Yang, Q. Qiu, T. Xie, and T. Liang. Application of Quantum Dot Interface Modification Layer in Perovskite Solar Cells : Progress and Perspectives. *Nanomaterials*, **12**(12):2102, (2022). DOI: https://doi.org/10.3390/nano12122102.

[70] O. Almora, C.I. Cabrera, J. Garcia-cerrillo, T. Kirchartz, U. Rau, and C.J. Brabec. Quantifying the Absorption Onset in the Quantum Efficiency of Emerging Photovoltaic Devices. *Adv. Energy Mater.*, **11**(16):2100022, (2021). DOI: https://doi.org/10.1002/aenm.202100022.

[71] V.P. Kamat, T. Kevin, and D. Baker. Interfacial Charge Transfer Dynamics in Quantum Dot Solar Cells. *ECS.*, **1**:1835–1835, (2011). DOI: https://doi.org/10.1149/MA2011-01/38/1835.

[72] Y. Zhang, G. Wu, F. Liu, C. Ding, Z. Zou, and Q. Shen. Photoexcited carrier dynamics in colloidal quantum dot solar cells : insights into individual quantum dots, quantum dot solid films and devices. *Chem. Soc. Rev.*, **49**:49–84, (2020). DOI: https://doi.org/10.1039/C9CS00560A.

[73] M. Jošt, L. Kegelmann, L. Korte, and S. Albrecht. Monolithic Perovskite Tandem Solar Cells : A Review of the Present Status and Advanced Characterization Methods Toward 30% Efficiency. *Adv. Energy Mater.*, **10**(26):1904102, (2020). DOI: https://doi.org/10.1002/aenm.201904102.

[74] M. Zhang, F. Guo, S. Lei, T. Zhong, B. Xiao, C. Liu, and L. Wang. Positive temperature dependence of the electroluminescent performance in a colloidal quantum dot light-emitting diode. *Dye. Pigment.*, **195**:109703, (2021). DOI: https://doi.org/10.1016/j.dyepig.2021.109703.

[75] B. Li, H. Di, B. Chang, R. Yin, et al. Efficient Passivation Strategy on Sn Related Defects for High Performance All-Inorganic $CsSnI_3$ Perovskite Solar Cells. *Adv. Funct. Mater.*, **31**(11):2007447, (2021). DOI: https://doi.org/10.1002/adfm.202007447.

[76] C.M. Chuang, P.R. Brown, V. Bulović, and M.G. Bawendi. Improved performance and stability in quantum dot solar cells through band alignment engineering. *Nature Materials*, **13**:796–801, (2014). DOI: https://doi.org/10.1038/nmat3984.

[77] H. Li, W. Shi, W. Huang, E.P. Yao, and J. Han. Carbon Quantum Dots/TiOx Electron Transport Layer Boosts Efficiency of Planar Heterojunction Perovskite Solar Cells to 19%. *Nano Lett.*, **17**(4): 2328–2335, (2017). DOI: https://doi.org/10.1021/acs.nanolett.6b05177.

[78] P. Caprioglio, M. Stolterfoht, C.M. Wolff, et al. On the Relation between the Open-Circuit Voltage and Quasi-Fermi Level Splitting in Efficient Perovskite Solar Cells. *Adv. Energy Mater.*, **9**(33): 1901631, (2019). DOI: https://doi.org/10.1002/aenm.201901631.

[79] Z. Zhu, J. Ma, Z. Wang, C. Mu, Z. Fan, et al. Efficiency enhancement of perovskite solar cells through fast electron extraction : The role of graphene quantum dots. . *J. Am. Chem. Soc.*, **136**(10):3760–3763, (2014). DOI: https://doi.org/10.1021/ja4132246.

[80] Y. Yuan, J. Ni, J. Yin, J. Guan, X. Zhou, et al. $CH_3NH_3PbBr_{3-x}I_x$ quantum dots enhance bulk crystallization and interface charge transfer for efficient and stable perovskite solar cells. *ACS Appl. Mater. Interfaces*, **12**(43):48861–48873, (2020). DOI: https://doi.org/10.1021/acsami.0c14191.

[81] L. Hu, W. Wang, H. Liu, J. Peng, H. Cao, et al. PbS colloidal quantum dots as an effective hole transporter for planar heterojunction perovskite solar cells. *J. Mater. Chem. A*, **3**(2):515–518, (2014). DOI: https://doi.org/10.1039/C4TA04272G.

[82] X. Zheng, N. Gasparini, O.F. Mohammed, H. Edward, O.M. Bakr, et al. Quantum Dots Supply Bulk- and Surface- Passivation Agents for Efficient and Stable Perovskite Solar Cells. *Joule*, **3**(8):1963–1976, (2019). DOI: https://doi.org/10.1016/j.joule.2019.05.005.

[83] S. Sidhik, J. Velusamy, and E.P.S.A. De. Role of carbon nanodots in defect passivation and photo-sensitization of mesoscopic-TiO_2 for perovskite solar cells. *Carbon*, **146**:388–398, (2019). DOI: https://doi.org/10.1016/j.carbon.2019.01.105.

[84] X. Chen, W. Xu, Z. Shi, G. Pan, J. Zhu, J. Hu, X. Li, C. Shan, and H. Song. Nano Energy Europium ions doped WO x nanorods for dual interfacial modification facilitating high efficiency and stability of perovskite solar cells. *Nano Energy*, **80**:105564, (2021). DOI: https://doi.org/10.1016/j.nanoen.2020.105564.

[85] Z. Yuan, Z. Wu, S. Bai, Z. Xia, W. Xu, and T. Song. Hot-Electron Injection in a Sandwiched TiOx-Au-TiOx Structure for High-Performance Planar Perovskite Solar Cells. *Adv. Energy Mater.*, **5**(10):1500038, (2015). DOI: https://doi.org/10.1002/aenm.201500038.

[86] P. Qin, T. Wu, Z. Wang, L. Xiao, L. Ma, F. Ye, and L. Xiong. Grain Boundary and Interface Passivation with Core - Shell Au@CdS Nanospheres for High-Efficiency Perovskite Solar Cells. *Adv. Funct. Mater.*, **30**(12):1908408, (2020). DOI: https://doi.org/10.1002/adfm.201908408.

[87] W. Hui, Y. Yang, Q. Xu, H. Gu, S. Feng, et al. Red-Carbon-Quantum-Dot-Doped SnO_2 Composite with Enhanced Electron Mobility for Efficient and Stable Perovskite Solar Cells. *Adv. Mater.*, **32**(4):1906374, (2020). DOI: https://doi.org/10.1002/adma.201906374.

[88] J. Xie, K. Huang, X. Yu, Z. Yang, K. Xiao, Y. Qiang, et al. Enhanced Electronic Properties of SnO_2 via Electron Transfer from Graphene Quantum Dots for Efficient Perovskite Solar Cells. *ACS Nano*, **11** (9):9176–9182, (2017). DOI: https://doi.org/10.1021/acsnano.7b04070.

[89] X. Zeng, T. Zhou, C. Leng, Z. Zang, et al. Performance Improvement of Perovskite Solar Cell by Employing CdSe Quantum Dot/PCBM Composite as Electron Transport Layer. *J. Mater. Chem A.*, **5**(33):1–3, (2017). DOI: https://doi.org/10.1039/C7TA00203C.

[90] P. Liu, Y. Sun, S. Wang, H. Zhang, Y. Gong, et al. Two dimensional graphitic carbon nitride quantum dots modified perovskite solar cells and photodetectors with high performances. *J. Power Sources*, **451**:227825, (2020). DOI: https://doi.org/10.1016/j.jpowsour.2020.227825.

[91] F. Gao, Q. Zheng, and Y. Zhang. Stability Improvement of Perovskite Solar Cells for Application of $CuInS_2$ Quantum Dot-Modi fied TiO_2 Nanoarrays. *ACS Omega*, **4**(2):3432–3438, (2019). DOI: https://doi.org/10.1021/acsomega.8b03629.

[92] H. Bian, D. Bai, J. Zhang, S.F. Liu, H. Bian, et al. Graded Bandgap $CsPbI_2$+xBr1Ax Perovskite Solar Cells with a Stabilized Efficiency of 14.4%. *Joule*, **2**(8):1500–1510, (2018). DOI: https://doi.org/10.1016/j.joule.2018.04.012.

[93] C. Chen, F. Li, L. Zhu, Z. Shen, Y. Weng, et al. Efficient and stable perovskite solar cells thanks to dual functions of oleyl amine-coated $PbSO_4(PbO)_4$ quantum dots : Defect passivation and moisture/oxygen blocking. *Nano Energy*, **68**:104313, (2020). DOI: https://doi.org/10.1016/j.nanoen.2019.104313.

[94] A. Sadhu, M. Rai, T. Salim, X. Jin, J. Ming, et al. Dual Role of Cu-Chalcogenide as Hole-Transporting Layer and Interface Passivator for p-i-n Architecture Perovskite Solar Cell. *Adv. Funct. Mater.*, **31** (38):2103807, (2021). DOI: https://doi.org/10.1002/adfm.202103807.

[95] S.M.H. Qaid, H.M. Ghaithan, B.A. Al-asbahi, and A.S. Aldwayyan. Investigation of the Surface Passivation Effect on the Optical Properties of $CsPbBr_3$ Perovskite Quantum Dots. *Surfaces and Interfaces*, **23**:100948, (2021). DOI: https://doi.org/10.1016/j.surfin.2021.100948.

[96] Z. Zhang, H. Song, W. Wang, H. Rao, Y. Fang, Z. Pan, and X. Zhong. Dual Ligand Capped Quantum Dots Improving Loading Amount for High- Efficiency Quantum Dot-Sensitized Solar Cells. *ACS Energy Lett.*, **8**(1):647–656, (2023). DOI: https://doi.org/10.1021/acsenergylett.2c02270.

[97] E. Khorshidi, B. Rezaei, D. Blätte, A. Buyruk, et al. Hydrophobic Graphene Quantum Dots for Defect Passivation and Enhanced Moisture Stability of $CH_3NH_3PbI_3$ Perovskite Solar Cells. *Sol. RRL*, **6**(7):2200023, (2022). DOI: https://doi.org/10.1002/solr.202200023.

[98] H. Liu, G. Jin, J. Wang, W. Zhang, L. Qing, et al. Quantum Dots Mediated Crystallization Enhancement in Two - Step Processed Perovskite Solar Cells. *Nano-Micro Lett.*, **17**:169, (2025). DOI: https://doi.org/10.1007/s40820-025-01677-5.

[99] P. Chawla, M. Ahamed, C. Sharma, and M. Kumar. A comparative study exploring the ligand binding capabilities of quarternary chalcopyrite copper indium gallium diselenide (CIGSe) nanocrystals. *J. Mol. Struct.*, **1245**:131055, (2021). DOI: https://doi.org/10.1016/j.molstruc.2021.131055.

[100] Q. Pan, Q. Zhao, P. Wei, and G. Li. Surface Ligands for Perovskite Quantum Dots. *ChemSusChem.*, **18**(4):202401875, (2025). DOI: https://doi.org/10.1002/cssc.202401875.

[101] Y. Bai, M. Hao, S. Ding, P. Chen, and L. Wang. Surface Chemistry Engineering of Perovskite Quantum Dots : Strategies, Applications and Perspectives. *Adv. Mater.*, **34**(4):2105958, (2022). DOI: https://doi.org/10.1002/adma.202105958.

[102] E. Zillner, P. Niyamakom, F. Rauscher, K. Ko, and T. Dittrich. Role of Ligand Exchange at CdSe Quantum Dot Layers for Charge Separation. *J. Phys. Chem. C.*, **116**(31):16747–16754, (2012). DOI: https://doi.org/10.1021/jp303766d.

[103] P. Tipparak, W. Passatorntaschakorn, W. Khampa, W. Musikpan, C.E. Usulor, et al. The Impact of $MAPbI_3$ Quantum Dots on CsFA Perovskite Solar Cells : Interface and Hole Extraction Improvement. *ACS Appl. Energy Mater*, **8**(1):355–365, (2025). DOI: https://doi.org/10.1021/acsaem.4c02474.

[104] H. Zhang, M.K. Nazeeruddin, and W.C.H. Choy. Perovskite Photovoltaics : The Significant Role of Ligands in Film Formation, Passivation, and Stability. *Adv. Mater.*, **31**(8):1805702, (2019). DOI: https://doi.org/10.1002/adma.201805702.

[105] A. Miglani, S.B. Ogale, and O.S. Game. Architectural Innovations in Perovskite Solar Cells. *Small*, **21**(15):2411355, (2025). DOI: https://doi.org/10.1002/smll.202411355.

[106] W. Chi and S.K. Banerjee. Performance Improvement of Perovskite Solar Cells by Interactions between Nano-Sized Quantum Dots and Perovskite. *Adv. Funct. Mater.*, **32**(28):2200029, (2022). DOI: https://doi.org/10.1002/adfm.202200029.

[107] C. Chen, H. Song, and C. Chen. Photon management to reduce energy loss in perovskite solar cells. *Chem. Soc. Rev.*, **50**:7250–7329, (2021). DOI: https://doi.org/10.1039/D0CS01488E.

[108] P. Kumar, R. Kumar, I.K. Iliev, H.I. Beloev, S. Praveenkumar, and N. Sunnam. Engineered Quantum Dot Solar Cells : From Fundamentals to Applications. *Plasmonic*, **20**:6887–6907, (2025). DOI: https://doi.org/10.1007/s11468-025-02915-7.

[109] P. Holzhey and M. Saliba. A full overview of international standards assessing the long-term stability of perovskite solar cells. *J. Mater. Chem. A*, **6**(44):21794–21808, (2018). DOI: https://doi.org/10.1039/C8TA06950F.

[110] P.M. Sommeling, M. Späth, H.J.P. Smit, N.J. Bakker, and J.M. Kroon. Long-term stability testing of dye-sensitized solar cells. *Journal of Photochemistry and Photobiology A: Chemistry*, **164**(3): 137–144, (2004). DOI: https://doi.org/10.1016/j.jphotochem.2003.12.017.

[111] T. Kim, B.S. Kim, J.G. Oh, S.C. Park, et al. Interfacial Engineering at Quantum Dot-Sensitized TiO_2 Photoelectrodes for Ultrahigh Photocurrent Generation. . *ACS Appl. Mater. Interfaces*, **13**(5): 6208–6218, (2021). DOI: https://doi.org/10.1021/acsami.0c19352.

[112] W. Hui, Y. Yang, Q. Xu, H. Gu, S. Feng, et al. Red-Carbon-Quantum-Dot-Doped SnO_2 Composite with Enhanced Electron Mobility for Efficient and Stable Perovskite Solar Cells. *Advanced Materials*, **32**(4):1906374, (2019). DOI: https://doi.org/10.1002/adma.201906374.

[113] X. Xia, D. Zhang, X. Wang, Z. Xiao, and F. Li. A carbon-quantum-dot-hybridized NiOx hole-transport layer enables efficient and stable planar p-i-n perovskite solar cells with high open-circuit voltage. *J. Mater. Chem. C.*, **9**(36):12213–12223, (2021). DOI: https://doi.org/10.1039/D1TC02595C.

[114] C. Qiu, Y. Wu, J. Song, W. Wang, and Z. Li. Efficient Planar Perovskite Solar Cells with ZnO Electron Transport Layer. *Coatings*, **12**(12):1981, (2022). DOI: https://doi.org/10.3390/coatings12121981.

[115] B. Li, D. Gao, S.A. Sheppard, W.D.J. Tremlett, et al. Highly Efficientand Scalable p-i-n Perovskite Solar Cells Enabledby Polymetallocene Interfaces. *J. Am.Chem.Soc.*, **146**(19):13391–13398, (2024). DOI: https://doi.org/10.1021/jacs.4c02220.

[116] S. Liu, Y. Lu, C. Yu, J. Li, R. Luo, R. Guo, et al. Triple-junction solar cells with cyanate in ultrawide-bandgap perovskites. *Nature*, **628**:306–312, (2024). DOI: https://doi.org/10.1038/s41586-024-07226-1.

[117] J.H. Heo and S.H. Im. $CH_3NH_3PbBr_3$-CH_3NH_3 PbI_3 Perovskite - Perovskite Tandem Solar Cells with Exceeding 2.2 V Open Circuit Voltage. *Ad. Materials.*, **28**(25):121–5125, (2015). DOI: https://doi.org/10.1002/adma.201501629.

[118] J. Wang, V. Zardetto, K. Datta, D. Zhang, M.M. Wienk, and R.A.J. Janssen. 6.8% Monolithic all-perovskite triple-junction solar cells via a universal two-step solution process. *Nat. Communications*, **11**:5254, (2020). DOI: https://doi.org/10.1038/s41467-020-19062-8.

[119] K. Xiao, J. Wen, Q. Han, R. Lin, Y. Gao, et al. Solution-Processed Monolithic All-Perovskite. *ACS Energy Lett.*, **5**(9):2819–2826, (2025). DOI: https://doi.org/10.1021/acsenergylett.0c01184.

[120] M. Jošt, E. Köhnen, A. Al-Ashouri, T. Bertram, et al. Perovskite/-CIGS Tandem Solar Cells: From Certified 24.2% toward 30% and beyond. *ACS Energy Lett.*, **7**(4):1298–1307, (2022).
DOI: https://doi.org/10.1021/acsenergylett.2c00274.

[121] Z. Wang, L. Zeng, T. Zhu, H. Chen, B. Chen, et al. Suppressed phase segregation for triple-junction perovskite solar cells. *Nature*, **618**:74–79, (2023).
DOI: https://doi.org/10.1038/s41586-023-06006-7.

[122] F. Xu, E. Aydin, H. Sargent, S. De Wolf, F. Xu, E. Aydin, et al. Monolithic perovskite/perovskite/silicon triple-junction solar cells with cation double displacement enabled 2.0 eV perovskites. *Joule*, **8**:224–240, (2024).
DOI: https://doi.org/10.1016/j.joule.2023.11.018.

[123] T. Chien, J. Yang, T. Kang, M. Fitzsimmons, G. Vega, et al. Incorporating thermal co-evaporation in current-matched all-perovskite triple-junction solar cells. *EES Sol.*, **1**:41–55, (2024).
DOI: https://doi.org/10.1039/D4EL00012A.

[124] D. Zhao, Y. Yu, C. Wang, W. Liao, N. Shrestha, et al. Low-bandgap mixed tin–lead iodide perovskite absorbers with long carrier lifetimes for all-perovskite tandem solar cells. *Nature Energy*, **2**:17018, (2017).
DOI: https://doi.org/10.1038/nenergy/.2017.18.

[125] D. Zhao, C. Wang, Z. Song, Y. Yu, C. Chen, X. Zhao, K. Zhu, and Y. Yan. Four-Terminal All-Perovskite Tandem Solar Cells Achieving Power Conversion Efficiencies Exceeding 23%. *ACS Energy Lett.*, **3**(2):305–306, (2018).
DOI: https://doi.org/10.1021/acsenergylett.7b01287.

[126] G. Kim, H. Min, K.S. Lee, D.Y. Lee, and S.M. Yoon. Impact of strain relaxation on performance of a -formamidinium lead iodide perovskite solar cells. . *Science*, **370**(6512):108–112, (2020).
DOI: https://doi.org/10.1126/science.abc4417.

[127] K. Xiao, R. Lin, Q. Han, Y. Hou, Z. Qin, H.T. Nguyen, et al. All-perovskite tandem solar cells with 24.2% certified efficiency and area over 1 cm^2 using surface-anchoring zwitterionic antioxidant. *Nat. Energy*, **5**:870–880, (2020).
DOI: https://doi.org/10.1038/s41560-020-00705-5.

[128] R. Lin, J. Xu, M. Wei, Y. Wang, Z. Qin, et al. All-perovskite tandem solar cells with improved grain surface passivation. *Nature*, **603**: 73–78, (2022).
DOI: https://doi.org/10.1038/s41586-021-04372-8.

[129] H. Chen, A. Maxwell, C. Li, S. Teale, B. Chen, T. Zhu, et al. Regulating surface potential maximizes voltage in all-perovskite tandems. *Nature*, **613**:676–681, (2023).
DOI: https://doi.org/10.1038/s41586-022-05541-z.

[130] H. Li, C. Ding, J. Wen, P. Wu, C. Liu, S. Zhao, and K. Xiao. All-perovskite tandem solar cells with 3D / 3D bilayer perovskite heterojunction. *Nature*, **620**:994–1000, (2023).
DOI: https://doi.org/10.1038/s41586-023-06278-z.

[131] X. Li, Z. Ying, S. Li, L. Chen, M. Zhang, and L. Liu. Top - Down Dual - Interface Carrier Management for Highly Efficient and Stable Perovskite / Silicon Tandem Solar Cells. *Nano-Micro Lett.*, **17**:141, (2025).
DOI: https://doi.org/10.1007/s40820-024-01631-x.

[132] H. Choi, S.U. Ryu, D.H. Lee, H. Kim, S. Song, H. Kim, and T. Park. Advancements in Organic-Based Hybrid Tandem Solar Cells Considering Light Absorption and Spectral Matching of Organic Materials. *ACS Energy Lett.*, **9**(6):3136–3168, (2024).
DOI: https://doi.org/10.1021/acsenergylett.4c01252.

[133] X. Tian, S.D. Stranks, and F. You. Life cycle energy use and environmental implications of high-performance perovskite tandem solar cells. *Sci. Adv.*, **6**(31):eabb0055, (2020).
DOI: https://doi.org/10.1126/sciadv.abb0055.

[134] D. Rosas-villalva, S. Zhumagali, B.K. Yildirim, A. Razzaq, and S. Sarwade. Enhanced cation interaction in perovskites for efficient tandem solar cells with silicon. *Science*, **385**(6708):533–538, (2024).
DOI: https://doi.org/10.1126/science.adp1621.

[135] M. Guo, W. Guo, J. Zhang, et al. Boosting Efficiency and Stability of Carbon Based Hole-Transport-Layer-Free Perovskite Solar Cells with the Additives of PbS Quantum Dots. *SSRN Electronic Journal*, **10**:3967340, (2021).

[136] Z. Luo, W. Yin, J. Wang, Y. Hua, Z. Zhou, et al. Quantum Dots Enable Perovskite Solar Cells Performance : Interactions, Mechanisms ,Progresses, and Future Perspectives. *Adv. Funct. Mater.*, **35** (20):2419268, (2025).
DOI: https://doi.org/10.1002/adfm.202419268.

[137] Q. Zhao, R. Han, A.R. Marshall, S. Wang, et al. Colloidal Quantum Dot Solar Cells : Progressive Deposition Techniques and Future Prospects on Large-Area Fabrication. *Adv. Mater.*, **34**(17):2107888, (2022).
DOI: https://doi.org/10.1002/adma.202107888.

[138] Q. Wei, D. Zheng, L. Liu, J. Liu, M. Du, L. Peng, and K. Wang. Fusing Science with Industry : Perovskite Photovoltaics Moving Rapidly into Industrialization. . *Adv. Mater.*, **36**(39):2406295, (2024).
DOI: https://doi.org/10.1002/adma.202406295.

[139] B. Sesha, S. Pokuri, J. Sit, O. Wodo, et al. Nanoscale Morphology of Doctor Bladed versus Spin-Coated Organic Photovoltaic Films. *Adv. Energy Mater.*, **7**(22):1701269, (2017).
DOI: https://doi.org/10.1002/aenm.201701269.

[140] E. Khorshidi, B. Rezaei, A. Kavousighahfarokhi, J. Hanisch, M.A. Reus, P. Mu, and T. Ameri. Antisolvent Additive Engineering for Boosting Performance and Stability of Graded Heterojunction Perovskite Solar Cells Using Amide-Functionalized Graphene Quantum Dots. *ACS Appl. Mater. Interfaces.*, **14**(49):54623–54634, (2022).
DOI: https://doi.org/10.1021/acsami.2c12944.

[141] J.A. Raiford, S.T. Oyakhire, and S.F. Bent. Applications of atomic layer deposition and chemical vapor deposition for perovskite solar cells. *Energy Environ. Sci.*, **13**:1997–2023, (2020).
DOI: https://doi.org/10.1039/D0EE00385A.

[142] S.S. Shin, S.J. Lee, and S. Il Seok. Metal Oxide Charge Transport Layers for Efficient and Stable Perovskite Solar Cells. *Adv. Funct. Mater.*, **29**(13):1900455, (2019).
DOI: https://doi.org/10.1039/D0EE00385A.

[143] V. Zardetto, B.L. Williams, A. Perrotta, F. Di Giacomo, et al. Sustainable Energy & Fuels research status, opportunities and challenges. *Sustainable Energy Fuels*, **1**:30–55, (2017).
DOI: https://doi.org/10.1039/C6SE00076B.

[144] Y. Weng, G. Chen, X. Zhou, and T. Yan, Q. Guo. Design and fabrication of bi-functional TiO_2/Al_2O_3 nanolaminates with selected light extraction and reliable moisture vapor barrier performance. *Nanotechnology*, **30**(8):085702, (2019).
DOI: https://doi.org/10.1088/1361-6528/aaf4e1.

[145] B. Gupta, A. Hossain, A. Riaz, A. Sharma, D. Zhang, et al. Recent Advances in Materials Design Using Atomic Layer Deposition for Energy Applications. *Adv. Funct. Mater.*, **32**(3):2109105, (2022).
DOI: https://doi.org/10.1002/adfm.202109105.

[146] Y. Cao, J. Xu, Z. Ge, Y. Zhai, W. Li, X. Jiang, and K. Chen. Energy conversion efficiency for hetero-junction. *J.Mater. Chem. C.*, **3**(46): 12061, (2015).
DOI: https://doi.org/10.1039/C5TC02585K.

[147] N. Shah, A.A. Shah, P.K. Leung, S. Khan, K. Sun, X. Zhu, and Q. Liao. A Review of Third Generation Solar Cells. *Processes*, **11** (6):1852, (2023).
DOI: https://doi.org/10.3390/pr11061852.

[148] N. Joseph, P. Ahmadiannamini, R. Hoogenboom, and I.F.J. Vankelecom. Layer-by-layer preparation of polyelectrolyte multilayer membranes for separation. *Polym. Chem.*, **5**(6):1817–1831, (2014). DOI: https://doi.org/10.1039/C3PY01262J.

[149] K.X. Steirer, J.J. Berry, M.O. Reese, and M.F.A.M. Van Hest. Ultrasonically sprayed and inkjet printed thin film electrodes for organic solar cells. . *Thin Solid Films*, **517**(8):2781–2786, (2009). DOI: https://doi.org/10.1016/j.tsf.2008.10.124.

[150] F. Aziz and A.F. Ismail. Materials Science in Semiconductor Processing Spray coating methods for polymer solar cells fabrication : A review. *Mater. Sci. Semicond. Process*, **39**:416–425, (2015). DOI: https://doi.org/10.1016/j.mssp.2015.05.019.

[151] X. Peng, J. Yuan, S. Shen, M. Gao, A.S.R. Chesman, and H. Yin. Perovskite and Organic Solar Cells Fabricated by Inkjet Printing : Progress and Prospects. *Adv. Funct. Mater.*, **27**(41):1703704, (2017). DOI: https://doi.org/10.1002/adfm.201703704.

[152] E. Smith, M. Fu, and K. Critchley. Inkjet printing of heavy-metal-free quantum dots-based devices : a review. *Nanotechnology*, **35**: 302002, (2024). DOI: https://doi.org/10.1088/1361-6528/ad40b3.

[153] A. Gusain. Roll-to-roll printing of polymer and perovskite solar cells : compatible materials and processes. *J. Mater. Sci.*, **55**:13490–13542, (2020). DOI: https://doi.org/10.1007/s10853-020-04883-1.

[154] J.E. Bishop, J.A. Smith, and D.G. Lidzey. Development of Spray-Coated Perovskite Solar Cells. *ACS Appl. Mater. Interfaces*, **12**(43): 48237–48245, (2020). DOI: https://doi.org/10.1021/acsami.0c14540.

[155] M. Eslamian. Spray-on Thin Film PV Solar Cells : Advances, Potentials and Challenges. *Coating*, **4**(1):60–84, (2014). DOI: https://doi.org/10.3390/coatings4010060.

[156] Y. Zhang, S. Ng, X. Lu, and Z. Zheng. Solution-Processed Transparent Electrodes for Emerging Thin-Film Solar Cells. *Chem. Rev.*, **120**(4):2049–2122, (2020). DOI: https://doi.org/10.1021/acs.chemrev.9b00483.

[157] X. Zhang, J. Zheng, Y. Wang, Z. Wang, and L. Zheng. Solvent-free synthetic protocols for halide perovskites. *Inorg. Chem. Front.*, **10**: 3468, (2023). DOI: https://doi.org/10.1039/D3QI00163F.

[158] I.M. Maafa. All-Inorganic Perovskite Solar Cells : Recent Advancements and Challenges. *Nanomaterials*, **12**(10):1651, (2022). DOI: https://doi.org/10.3390/nano12101651.

[159] M. Wang and C.J. Carmalt. Film Fabrication of Perovskites and their Derivatives for Photovoltaic Applications via Chemical Vapor Deposition. *ACS Appl. Energy Mater.*, **5**(5):5434–5448, (2022). DOI: https://doi.org/10.1021/acsaem.1c02612.

[160] A. Khorasani, F. Mohamadkhani, M. Marandi, H. Luo, and M. Abdijalebi. Opportunities, Challenges, and Strategies for Scalable Deposition of Metal Halide Perovskite Solar Cells and Modules. *Adv. Energy Sustainability Res.*, **5**(7):2300275, (2024). DOI: https://doi.org/10.1002/aesr.202300275.

[161] H. Chen, X. Ding, P. Xu, T. Hayat, A. Alsaedi, J. Yao, Y. Ding, and S. Dai. Forming Intermediate Phase on the Surface of PbI_2 Precursor Films by Short-time DMSO Treatment for High-efficiency Planar Perovskite Solar Cells via Vapor-assisted Solution Process. *ACS Appl. Mater. Interfaces.*, **10**(2):1781–1791, (2018). DOI: https://doi.org/10.1021/acsami.7b17781.

[162] F. Fu. Triple-cation perovskite solar cells fabricated by a hybrid PVD/blade coating process using green solvents. *J. Mater. Chem. A.*, **9**:26680, (2021). DOI: https://doi.org/10.1039/D1TA07579A.

[163] B. Wilk, S. Sahayaraj, V. Babu, et al. Inkjet Printing of Quasi-2D Perovskite Layers with Optimized Drying Protocol for Efficient Solar Cells. . *Adv. Mater. Technol.*, **7**(12):2200606, (2022). DOI: https://doi.org/10.1002/admt.202200606.

[164] L. Tan, H. Jiang, R. Yang, L. Shen, C. Sun, Y. Jin, and X. Guan. Quantitative Surface Passivation Through Drop-on-Demand Inkjet Printing Enables Highly Efficient Perovskite Solar Cells. . *Adv. Energy Mater.*, **14**(7):2400549, (2024). DOI: https://doi.org/10.1002/aenm.202400549.

[165] M. Hçsel, H.F. Dam, and F.C. Krebs. Development of Lab-to-Fab Production Equipment Across Several Length Scales for Printed Energy Technologies . *Including Solar Cells. Energy Technol.*, **3** (4):293–304, (2015). DOI: https://doi.org/10.1002/ente.201402140.

[166] A. Kumar, S.K. Tripathi, M. Shkir, S. Alfaify, and T. Srilavanya. Processing methods towards scalable fabrication of perovskite solar cells : A brief review. *Inorg. Chem. Commun.*, **169**:113115, (2024). DOI: https://doi.org/10.1016/j.inoche.2024.113115.

[167] N. Samantaray, B. Parida, T. Soga, A. Sharma, A. Kapoor, A. Najar, and A. Singh. Recent Development and Directions in Printed Perovskite Solar Cells. . *Phys. Status Solidi A.*, **219**(6):2100629, (2022). DOI: https://doi.org/10.1002/pssa.202100629.

[168] S.G. Torres. Doctoral thesis Inkjet printing next-generation flexible devices : memristors. *photodetectors and perovskite LEDs Directors*, , (2024).

[169] S. Bhattarai, D. Borah, J. Rout, R. Pandey, J. Madan, et al. Designing an efficient lead-free perovskite solar cell with green-synthesized $CuCrO_2$ and CeO_2 as carrier transport materials. *RSC Adv.*, **13**:34693–34702, (2023). DOI: https://doi.org/10.1039/D3RA06722J.

[170] Q. Tai, K. Tang, and F. Yan. Recent progress of inorganic perovskite solar cells. . *Energy Environ. Sci.*, **12**(8):2375, (2019). DOI: https://doi.org/10.1039/C9EE01479A.

[171] R. Abargues, J. Navarro, P.J. Rodríguez-Cantó, et al. Enhancing the photocatalytic properties of PbS QD solids : the ligand exchange approach. *Nanoscale*, **11**(4):1978–1987, (2019). DOI: https://doi.org/10.1039/C8NR07760F.

[172] P. Zhang, G. Yang, F. Li, J. Shi, and H. Zhong. Direct in situ photolithography of perovskite quantum dots based on photocatalysis of lead bromide complexes. *Nature Commun.*, **13**:6713, (2022). DOI: https://doi.org/10.1038/s41467-022-34453-9.

[173] K.M. Salim, S. Masi, A.F. Gualdron-Reyes, R.S. Sanchez, et al. Boosting Long-Term Stability of Pure Formamidinium Perovskite Solar Cells by Ambient Air Additive Assisted Fabrication. *ACS Energy Lett.*, **6**(10):3511–3521, (2021). DOI: https://doi.org/10.1021/acsenergylett.1c01311.

[174] M.A. Siguan, D. Becker-Koch, A.D. Taylor, Q. Sun, et al. Efficient and Stable PbS Quantum Dot Solar Cells by Triple-Cation Perovskite Passivation. *ACS Nano.*, **14**(1):384–393, (2020). DOI: https://doi.org/10.1021/acsnano.9b05848.

[175] Y. Wang, N. Ding, D. Zhou, W. Xu, R. Sun, et al. ZnS-coated Yb^{3+}-doped perovskite quantum dots : A stable and efficient quantum cutting photon energy converter for silicon-based electronics. *Che. Eng. Journal.*, **487**:150347, (2024). DOI: https://doi.org/10.1016/j.cej.2024.150347.

[176] Md.H. Miah, Md.B. Rahman, M. Nur-E-Alam, et al. Key degradation mechanisms of perovskite solar cells and strategies for enhanced stability: issues and prospects. *RCS Adv.*, **15**:628–654, (2025). DOI: https://doi.org/10.1039/D4RA07942F.

[177] N. Shanmugam, R. Pugazhendhi, and R.M. Elavarasan. Anti-Reflective Coating Materials : A Holistic Review from PV Perspective. *Energies*, **13**(10):2631, (2020). DOI: https://doi.org/10.3390/en13102631.

[178] J. Khan, I. Ullah, and J. Yuan. $CsPbI_3$ perovskite quantum dot solar cells: opportunities, progress and challenges. *Materials Advances*, **3**:1931–1952, (2022).
DOI: https://doi.org/10.1039/D1MA01075A.

[179] C. Bathula, T. Nath Mandal, S. Naik, A. Meena, A. Nesargi, and A. Jana. Synthesis, characterization, and optical studies of lead-free perovskite, $Cs_3M_2Br_9$ (M = Bi, Sb) nanocrystals. *Inorg. Chem. Commun.*, **165**:112516, (2024).
DOI: https://doi.org/10.1016/j.inoche.2024.112516.